

Copyright Warning & Restrictions

The copyright law of the United States (Title 17, United States Code) governs the making of photocopies or other reproductions of copyrighted material.

Under certain conditions specified in the law, libraries and archives are authorized to furnish a photocopy or other reproduction. One of these specified conditions is that the photocopy or reproduction is not to be “used for any purpose other than private study, scholarship, or research.” If a user makes a request for, or later uses, a photocopy or reproduction for purposes in excess of “fair use” that user may be liable for copyright infringement,

This institution reserves the right to refuse to accept a copying order if, in its judgment, fulfillment of the order would involve violation of copyright law.

Please Note: The author retains the copyright while the New Jersey Institute of Technology reserves the right to distribute this thesis or dissertation

Printing note: If you do not wish to print this page, then select “Pages from: first page # to: last page #” on the print dialog screen

The Van Houten library has removed some of the personal information and all signatures from the approval page and biographical sketches of theses and dissertations in order to protect the identity of NJIT graduates and faculty.

ABSTRACT

DEVELOPMENT OF A DEVICE FOR WHOLE BODY STIMULATION OF THE OTOLITHS

**by
Jon Edward Weimer**

Over the past few decades, research has been conducted to explore the effects of microgravity on human musculature. As seen in astronauts upon their return to Earth after prolonged spaceflight, extensive muscle atrophy due to adaptation to conditions of microgravity many times decreases a person's ability to walk or even stand. With an understanding of the anatomical mechanisms that provide postural control, the proper stimulation, resulting in a reduction in spasticity, could be provided by simulating these conditions of microgravity.

In order to simulate microgravity, a device has been developed that is capable of providing whole body stimulation of the otoliths. The design of this device is presented in detail in this thesis along with its performance characteristics. When subjected to the vestibular stimulation that this device will provide, persons will theoretically experience a reduction in spasticity. Therefore, this device allows spasticity to be explored further in the future.

**DEVELOPMENT OF A DEVICE FOR WHOLE
BODY STIMULATION OF THE OTOLITHS**

by
Jon Edward Weimer

**A Thesis
Submitted to the Faculty of
New Jersey Institute of Technology
in Partial Fulfillment of the Requirements for the Degree of
Master of Science in Biomedical Engineering**

Department of Biomedical Engineering

January 2010

Blank Page

APPROVAL PAGE

**DEVELOPMENT OF A DEVICE FOR WHOLE
BODY STIMULATION OF THE OTOLITHS**

Jon Edward Weimer

Dr. Richard A. Foulds, Thesis Advisor
Associate Professor of Biomedical Engineering, NJIT

12/7/09

Date

Dr. Sergei Adamovich, Committee Member
Associate Professor of Biomedical Engineering, NJIT

12/3/09

Date

Dr. Bruno A. Mantilla, Committee Member
University Lecturer of Biomedical Engineering, NJIT

12/3/09

Date

BIOGRAPHICAL SKETCH

Author: Jon Edward Weimer

Degree: Master of Science

Date: January 2010

Undergraduate and Graduate Education:

- Master of Science in Biomedical Engineering,
New Jersey Institute of Technology, Newark, NJ, 2010
- Bachelor of Science in Mechanical Engineering,
Purdue University, West Lafayette, IN, 2008

Major: Biomedical Engineering

ACKNOWLEDGMENT

I would like to express my deepest gratitude to my advisor, Dr. Richard Foulds, who provided me not only with the necessary funds to complete this thesis, but more importantly with guidance, support, and insight. I would also like to give thanks to Dr. Sergei Adamovich and Dr. Bruno Mantilla for actively participating on my committee and supporting me throughout this process. A special thank you is extended to John Hoinowski for continually giving his invaluable time and effort to provide the necessary machining expertise to successfully complete the construction of this device.

I am much appreciative for the support and encouragement of my colleagues I have been associated with during this portion of my academic career: Kai Chen, Megan Damcott, Amanda Irving, Brooke Odle, Diego Ramirez, Mark Shaker, Darnell Simon, and Katherine Swift. Special thanks to Jenine Draughon and Candida Rocha for assisting with the purchasing of parts for this device.

Finally, I would like to thank my parents, Paul and Glenda, for the never-ending love, guidance, and support they have given me throughout my life. With regards to the design of this device, numerous improvements were sparked through collaborations with my father. By believing in me, my parents have taught me to believe in myself and strive for greatness.

TABLE OF CONTENTS

Chapter	Page
1 INTRODUCTION.....	1
1.1 Objective.....	1
1.2 Background.....	1
1.2.1 Understanding Spasticity.....	2
1.2.2 Reduced Muscle Tone from Microgravity.....	2
1.2.3 The Otoliths – Sensing Gravity.....	4
2 STIMULATING THE OTOLITHS.....	9
2.1 Simulation of Microgravity.....	9
2.2 Therapeutic Interventions.....	10
2.2.1 Rotary Motion Stimulation.....	10
2.2.2 Vertical, Linear Motion Stimulation.....	14
2.2.3 Important Experimental Testing Conditions.....	15
3 DEVELOPMENT OF THE DEVICE.....	17
3.1 Product Design Specifications.....	17
3.2 Preliminary Design Calculations.....	19
3.2.1 Required Lifting Force.....	20
3.2.2 Time for Free-Fall.....	22
3.2.3 Choosing a Pneumatic Air Cylinder.....	23
3.2.4 Air Compressor Requirements.....	24
3.3 Technical Product Specifications.....	25

TABLE OF CONTENTS
(Continued)

Chapter	Page
4 DEVICE PERFORMANCE RESULTS.....	39
5 CONCLUSIONS AND FURTHER IMPROVEMENTS.....	49
APPENDIX A CONTROL VALVE SPECIFICATIONS.....	51
APPENDIX B NI DAQCARD-6024E SPECIFICATIONS.....	54
APPENDIX C NI DAQCARD-6024E ACCESSORIES SPECIFICATIONS.....	57
APPENDIX D REED RELAY SPECIFICATIONS.....	59
APPENDIX E PNEUMATIC AIR CYLINDER SPECIFICATIONS.....	60
APPENDIX F BILL OF MATERIALS.....	64
APPENDIX G MACHINED PART DRAWINGS.....	68
APPENDIX H MATLAB CODE.....	78
REFERENCES.....	81

LIST OF TABLES

Table	Page
3.1 Upward Acceleration (ft/s ²) of a 275 lbf by a Single Pneumatic Air Cylinder...	21
3.2 Air Expulsion Rate (SCFM) from an Air Cylinder for a Four Inch Free-Fall...	23
3.3 Upward Acceleration (ft/s ²) of a 275 lbf by Four Pneumatic Air Cylinders.....	24
B.1 National Instruments DAQCard-6024E Analog I/O Specifications.....	54
B.2 National Instruments DAQCard-6024E Digital I/O Specifications.....	55
B.3 National Instruments DAQCard-6024E Counter/Timers Specifications.....	56
D.1 Compact 5VDC/1A SPST Reed Relay General Features.....	59
D.2 Compact 5VDC/1A SPST Reed Relay Technical Specifications.....	59
E.1 Dimension Values for Bimba Position Feedback Cylinder.....	61
E.2 Wiring Chart for Position Feedback Cylinders.....	62
F.1 Bill of Materials.....	64
G.1 Parts Requiring Additional Machining.....	68

LIST OF FIGURES

Figure		Page
1.1	Size of the calf muscles in humans as a function of bed-rest duration.....	4
1.2	Orientation of the otolith organs in the inner ear of the human head.....	5
1.3	Anatomy of the otolith organs.....	6
1.4	Mechanism by which the otolith organs sense translations and linear accelerations.....	7
1.5	Gravitational effects on the saccule and its impact on neural firing.....	8
2.1	Seesaw otolith stimulation device.....	11
2.2	Motion of the otolith organs.....	12
2.3	Position and acceleration data collected for rotary otolith stimulation device..	13
2.4	Knee trajectories collected during pre and post-stimulation LDPT for rotary otolith stimulation device.....	14
2.5	Leg drop pendulum test results showing effects of vertical, whole body stimulation of the otoliths.....	15
3.1	Otolith stimulation platform base.....	26
3.2	Otolith stimulation platform mobile frame.....	27
3.3	Otolith stimulation base frame with guide blocks, rails, and actuators.....	28
3.4	Position and acceleration data collected for stimulation platform without pneumatic system attached.....	29
3.5	Pneumatic system schematic.....	30
3.6	Electrical system diagram.....	31
3.7	Breadboard with reed relays.....	32
3.8	Close-up of relay connections.....	33
3.9	CB-68LP connection block.....	33

**LIST OF FIGURES
(Continued)**

Figure	Page
3.10 Close-up of DIO0 and DIO1 connection block ports.....	34
3.11 Final lowered assembly model.....	35
3.12 Final raised assembly model.....	35
3.13 Final device in lowered position.....	36
3.14 Final device in raised position.....	37
3.15 Otolith stimulation platform with chair designed for LDPT.....	38
4.1 180 pound person sitting in chair attached to device following stimulation....	39
4.2 Position, velocity, and acceleration data collected for a 180 pound person.....	40
4.3 Position, velocity, and acceleration data collected for a 90 pound person.....	41
4.4 Position, velocity, and acceleration data collected for zero load.....	42
4.5 90 pound load added to otolith stimulation device.....	42
4.6 Otolith stimulation device with no additional loading.....	43
4.7 Portion of position, velocity, and acceleration data collected for zero load.....	45
4.8 Portion of position data collected for zero load	46
4.9 Position, velocity, and acceleration data collected for zero load without applying an upward air pressure to catch the free-fall.....	47
4.10 Position data collected for zero load without applying an upward air pressure to catch the free-fall.....	48
A.1 Isonic MOD3 valve data.....	51
A.2 Isonic MOD3 manifold and wiring information.....	52
A.3 Alkon Corporation series P 3-way control valve specifications.....	53

LIST OF FIGURES
(Continued)

Figure	Page
C.1 National Instruments SH68-68-EP cable I/O connector diagram.....	57
C.2 National Instruments CB-68LP connection block layout.....	58
E.1 Pneumatic actuator with assigned dimension variables.....	60
E.2 Engineering specifications for position feedback cylinders.....	63
G.1 Horizontal support tube #1 drawing.....	69
G.2 Horizontal support tube #2 drawing.....	70
G.3 Horizontal support tube #3 drawing.....	71
G.4 Horizontal mounting tube drawing.....	72
G.5 Vertical support tube #1 drawing.....	73
G.6 Vertical support tube #2 drawing.....	74
G.7 Vertical mounting tube drawing.....	75
G.8 Connecting tube drawing.....	76
G.9 Piston mounting bracket drawing.....	77

CHAPTER 1

INTRODUCTION

1.1 Objective

The objective of this thesis is to present the development of a device for whole body stimulation of the otoliths. Over the past few decades, similar devices have been developed and used experimentally to explore muscular changes due to linear and angular accelerations. This device was developed in support of the research currently being conducted in the Rehabilitation Engineering Research Center on Technology for Children with Orthopedic Disabilities at New Jersey Institute of Technology. This research, titled “Toward a New Understanding of Spasticity”, is devoted to gaining an understanding of the roles of spasticity and motor control in limiting the function of children with cerebral palsy and traumatic brain injury.

1.2 Background Information

For decades, various forms of whole body motion have been used in treatment regimes for persons with cerebral palsy. In addition, a vast array of experimental research has been conducted to explore the effects of these motions on human physiology. The findings have been bountiful and have continually provided new platforms for further research. The therapies incorporating this idea of whole body motion are generally said to be providing “vestibular stimulation” [1].

1.2.1 Understanding Spasticity

Cerebral palsy (CP) is an abnormality of motor function and postural tone that is acquired at an early age. A common condition associated with cerebral palsy, among other disorders, is spasticity. Spasticity is a state of increased tone of a muscle, thus resulting in the deep tendon reflexes. This increase in tone causes the muscle to feel tight and rigid, thus resulting in an exaggerated knee jerk reflex, among other exaggerated reflexes. There are two components of muscle spasticity: neural and mechanical. In individuals with spasticity, resistance to passive movement has been suggested to be due to both the neural mechanisms and mechanical properties of muscle. This thesis focuses on the neural mechanisms and how a specific stimulation can alter the descending neural signals that in turn lead to a reduction in spasticity.

1.2.2 Reduced Muscle Tone from Microgravity

On Earth, humans are constantly exposed to the downward force of gravity, which is equivalent to an upward acceleration. In the absence of other linear accelerations, this provides a stable vertical reference. During translational head motion, the otolith organs, the saccule and utricle, sense both linear and centripetal accelerations [2]. Linear acceleration in the vertical direction is the focus of this thesis.

Spaceflight has led to expansive research related to the effects of microgravity on the musculoskeletal system. The knowledge gained from this research has allowed for expansive research to be conducted with regards to spasticity and other musculature disorders. In the absence of gravitational load, skeletal muscle atrophies. Reductions in peak force and velocity of contraction have been observed [3]. This absence of gravitational load has come to be referred to as microgravity. Another term,

weightlessness, is a feeling that is felt by an astronaut, or any person in free-fall. It is a feeling that is temporarily felt at moments while riding a rollercoaster or in a briskly descending elevator. During spaceflight, this feeling is experienced by astronauts; however, due to small perturbations (i.e. vibrations and local gravitational effects) during spaceflight, astronauts do not experience perfect weightlessness and therefore, microgravity has come to be used to describe the state of near weightlessness associated with spaceflight and free-fall [3].

The effects of microgravity on postural control have been studied over time. In postural studies discussed by Clement [4], spaceflight experiments have shown that by attaching an astronaut's feet to the deck of the spacecraft leads to greater flexion of the knees and trunk in comparison to that on Earth. This, among other observations [5,6], suggest that prolonged exposure to microgravity induces a gradual alteration of muscle signals [7]. The length of exposure to microgravity is a contributing factor in the reduction in muscle tone. Similarly, upon returning to Earth's gravitational forces, a person's muscle tone will gradually return to normal over time. This has been shown in post-flight studies of posture and locomotion [8,9,10].

Human and animal studies continually provide results with evidence of substantial muscle atrophy following simulated or actual microgravity conditions. This is due to the decreasing size of the muscle fibers and not the quantity of muscle fibers present. Studies have also shown that atrophy is greater for muscles required for postural control when compared to other muscles of the physiological system [11]. Figure 1.1 supports the conclusion that microgravity leads to muscle atrophy by providing evidence of this

occurring in humans subjected to bed rest. The mechanisms behind this muscle atrophy are discussed in the following section.

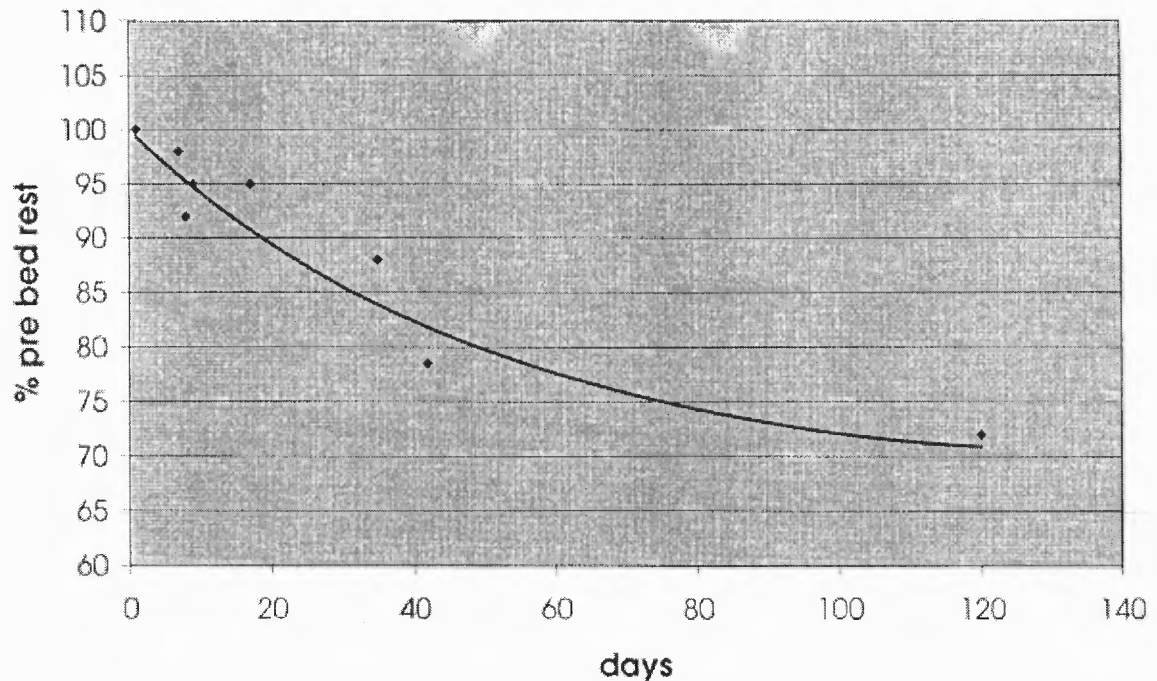


Figure 1.1 Size of the calf muscles (percent of initial value) in humans as a function of bed-rest duration (days). [11]

1.2.3 The Otoliths – Sensing Gravity

The vestibular system consists of two parts: the otolith organs and the semicircular canals. The semicircular canals detect the head's angular acceleration and thus are not of concern for this thesis. However, the otolith organs have two functions, to sense the head's linear acceleration and the head's position relative to gravity. In order to understand the mechanisms controlling the functions above, it is necessary to gain an understanding of the anatomy of the otolith organs. The otolith organs are two membranous sacs, the utricle and the saccule, within the inner ear. Figure 1.2, below, shows the orientation of the utricle and saccule. With the head upright, the utricle senses translations in the horizontal plane (left/right and forward/backward, while the saccule

senses translations in the vertical plane (up/down and forward/backward). The macula of the utricle projects downward, while the macula of the saccule projects sideways. Figure 1.3 represents the anatomy of the otolith organs. All components of the otolith organs play very important roles for postural control.

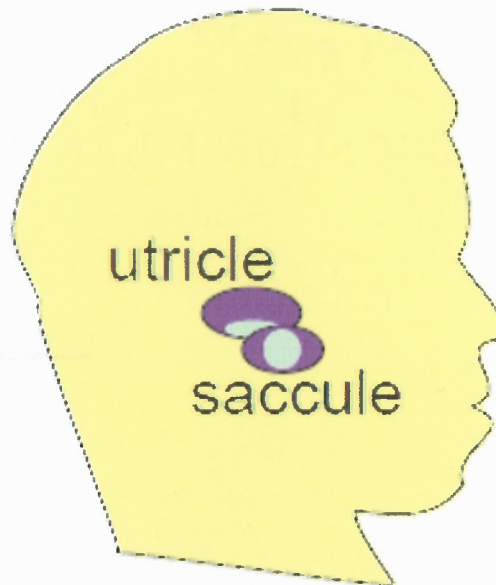


Figure 1.2 Orientation of the otolith organs in the inner ear of the human head. The utricle is oriented horizontally for sensing translations in the horizontal plane. The saccule is oriented vertically for sensing translations in the vertical plane (i.e., translations due to gravity). [12]

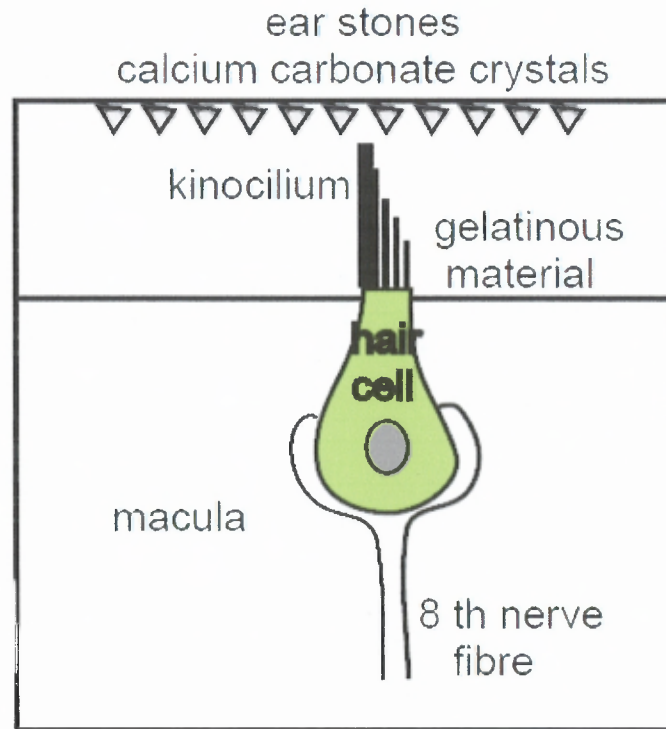


Figure 1.3 Anatomy of the otolith organs. Within each organ, the macula contains hair cells innervated by neurons of the 8th nerve. The hair cells project into a gelatinous material, represented as the upper region of the figure. Embedded within the gelatinous substance are calcium carbonate crystals. In addition, the stereocilia extend into the gel, the largest and thickest being the kinocilium. [12]

For this thesis, the device was designed to be used in conjunction with a specially designed chair that would be attached to the platform, with the intentions of the subjects to be sitting with their heads upright at all times. Therefore, only the function of the saccule is of true interest. For the purpose of understanding how the saccule senses vertical translations, it is easier to look at the utricle, where horizontal translations are detected and gravitational effects are not present. Figure 1.4 displays this phenomenon. The crystals provide an inertia that bends the hair cells in the opposite direction of the motion of the head. When the stereocilia bend toward the kinocilium, an increase in action potential frequency occurs in the 8th nerve afferents. In contrast, when the

stereocilia bend away from the kinocilium, a decrease in action potential frequency occurs.

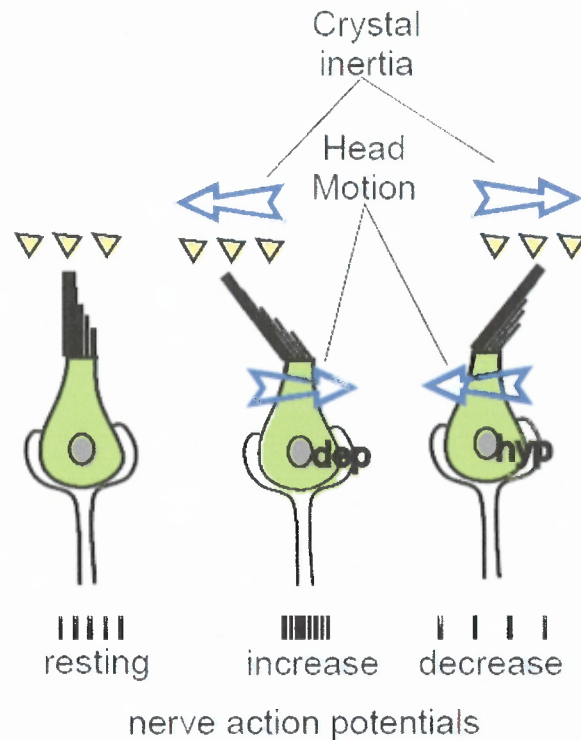


Figure 1.4 Mechanism by which the otolith organs sense translations and linear accelerations. The figure on the left represents the resting state in which no motion occurs and thus no inertial effects are present. The middle and right figures display the effects due to translational movement toward and away from the kinocilium. [12]

Now, with an understanding of the underlying mechanisms involved in detecting translational motion, it is important to apply this to the saccule. The saccule functions with the same mechanisms as the utricle; however, with the head upright, the crystals are affected by Earth's gravitational field in the saccule. In the resting state, the hairs are bent downward toward the kinocilium because of gravity and thus an increase in the action potential frequency in the 8th nerve afferents occurs. This is shown in Figure 1.5.

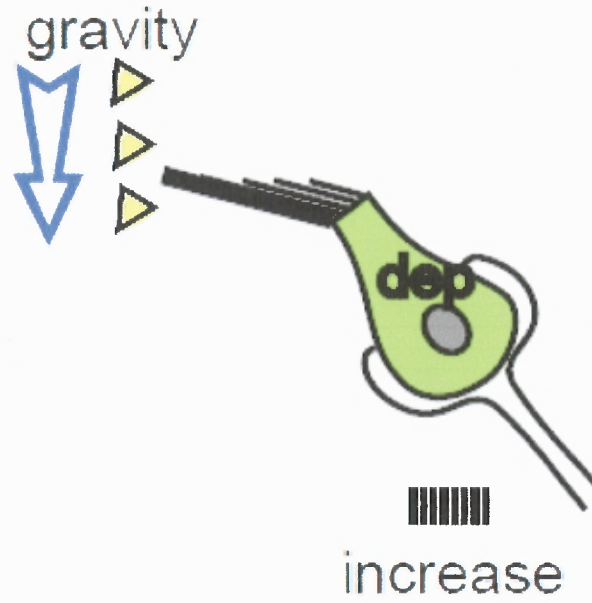


Figure 1.5 Gravitational effects on the saccule and its impact on neural firing. This figure represents the saccule in its resting state in which no motion occurs and thus the only effect present is gravity. [12]

Considering a person in free-fall, due to the person being subjected to a downward linear acceleration equal to the acceleration due to gravity, they would experience a feeling of microgravity and the hair cells would not bend, thus causing a reduction in the action potential frequency in the 8th nerve afferents. With that in mind, a greater reduction could be achieved by subjecting the person to a linear acceleration greater than the acceleration due to gravity. The goal of this device is to be capable of producing a downward linear acceleration equal to the acceleration due to gravity, thus leading to reduced neural firing, which in turn will lead to a reduction in spasticity.

CHAPTER 2

STIMULATING THE OTOLITHS

2.1 Simulation of Microgravity

Microgravity, as experienced during spaceflight, is difficult to simulate on Earth, especially for the prolonged periods of time necessary to detect changes in the musculoskeletal system. However, through various strategies, the effects on the musculoskeletal system from microgravity can be simulated. Kirsch and Gunga [11] briefly discuss three of these techniques that allow for simulated conditions of muscle unloading in which weight-bearing is prevented. These interventions are listed as follows:

1. Bed rest
2. Lower-limb suspension
3. 'Dry water-immersion'

For the bed rest technique, healthy subjects are confined in bed and typically have their head tilted downward 6 degrees to allow for simulation of the fluid shifts that occur in space. As for the lower-limb suspension strategy, one leg is unloaded by means of appropriate straps and/or through elevation of the sole of the contra-lateral shoe. During 'dry water-immersion', healthy subjects are immersed in water from which they are separated by means of a layer of impermeable tissue. They become virtually completely buoyant, which supports their body weight. However, during this intervention, the subjects remain dry and are thereby capable of being subjected to long periods of immersion [11].

Although all of these techniques are good for simulating weightless conditions, none of these techniques do so by stimulating the otolith organs. In fact, during bed rest, the otolith organ of interest, the saccule, is not even in the correct orientation to simulate free-fall of a person with their head in the upright position. The utricle is sensing gravity when a person is lying down in bed. Due to these reasons, none of these techniques are appropriate as interventions that will allow for tracking of musculoskeletal responses to stimulation of the saccule. A very specific intervention needs to be employed and thus a new device has been developed to provide proper stimulation to the saccule.

2.2 Therapeutic Interventions

For decades, a number of interventions have been used in therapeutic treatment programs for individuals with cerebral palsy. These treatment strategies have been reported to have contributed to an array of quantitatively and qualitatively measurable benefits and improvements in individuals with spastic cerebral palsy.

2.2.1 Rotary Motion Stimulation

Rotary and rocking motions have been incorporated into such treatment programs and have shown benefits such as improvements in alignment, improvements in balance reactions, and normalization of tone [13,14,15]. In addition, therapeutic horseback riding (hippo therapy) has been observed to provide anecdotal evidence of decreased spasticity of the legs, increased relaxation effects, and improved trunk and postural control [1]. Donahue [16] observed the same benefits from hippo therapy as observed from rotary and rocking motion stimulation. As observed by Fee [1], hippo therapy provides

vestibular stimulation that consists of a combination of both horizontal and vertical movements, with the vertical component having the greatest prevalence.

Prior to designing the otolith stimulation platform, a device was constructed and used to provide vestibular stimulation to subjects with spasticity. The device was twelve feet long with a fulcrum in the center, and so inherently the device was a seesaw. A chair designed for performing the passive leg drop pendulum test (LDPT), as first devised by Wartenburg [17], was attached to one end as shown in Figure 2.1.



Figure 2.1 Seesaw otolith stimulation device. Displayed is half of the device, including the chair and fulcrum.

In order to determine the performance results of the device, a three-dimensional camera motion capture system was utilized. With consideration of the proximity of the otolith organs of a person sitting in the chair, a marker was placed in this region and the device performance data was collected. Figure 2.2 shows the motion of this point, while

Figure 2.3 displays the vertical position and acceleration of this point. As shown in Figure 2.2, the motion consists of both horizontal and vertical components. During the motion, the point displaces approximately seven inches vertically and eight inches horizontally. Likewise, Figure 2.3 shows a seven inch range of vertical motion with approximately five inches of that range consisting of unrestrained motion. The final two inches of displacement occur while the device is being cushioned. Also, shown in Figure 2.3, is that the vertical acceleration of the point representing the otoliths is approximately half of the acceleration due to gravity.

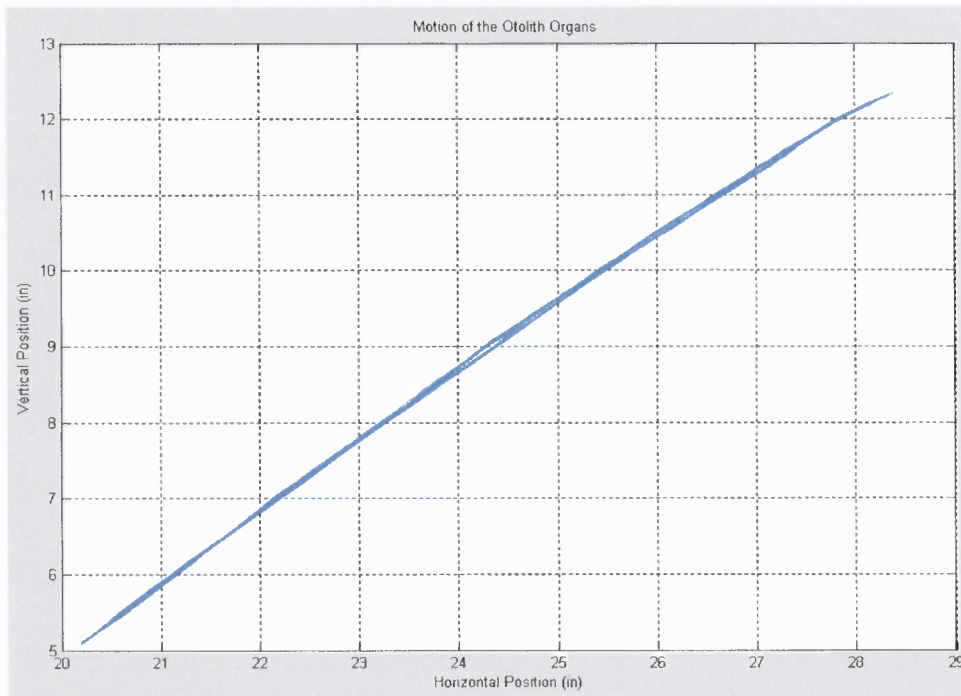


Figure 2.2 Motion of the otolith organs.

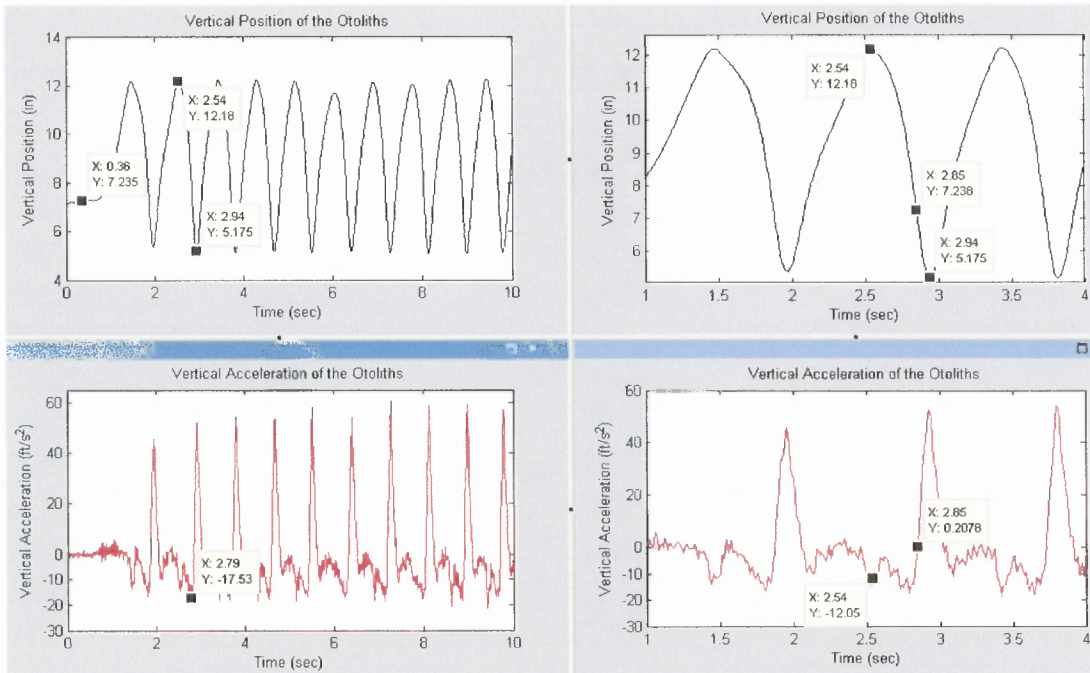


Figure 2.3 Position and acceleration data collected for rotary otolith stimulation device.

A quick study was conducted to determine if the rotary motion device provided the proper vestibular stimulation that would lead to a reduction in spasticity. A male adult with cerebral palsy was subjected to fifteen minutes of stimulation with this device and the leg drop pendulum test was repeatedly performed on the subject prior to and following the test. Shown in blue, in Figure 2.4, is a pre-stimulation knee trajectory curve representative of all of the samples prior to stimulation. Likewise, shown in red is a post-stimulation knee trajectory curve representative of all of the samples following stimulation.

Comparing the two knee trajectories, it is evident that the frequency of the oscillations decreases following vestibular stimulation. From the first two oscillations, it is also recognizable that the amplitude of the knee motion increases following stimulation. It is important to note that both trajectories began and ended at approximately the same angle. Since frequency of oscillation is proportional to stiffness,

while mass remains constant, it can be concluded that the vestibular stimulation led to a decrease in muscle stiffness. Also, since damping is inversely proportional to amplitude, it can be concluded that the stimulation from the device caused a decrease in the damping characteristics of the muscle. One final observation was that following stimulation, the knee angle during the initial swing of the leg surpassed its resting state. This did not occur until the fourth swing prior to stimulation. In summary, the rotary motion otolith stimulation device caused a decrease in muscle stiffness and damping for the subject with spastic cerebral palsy.

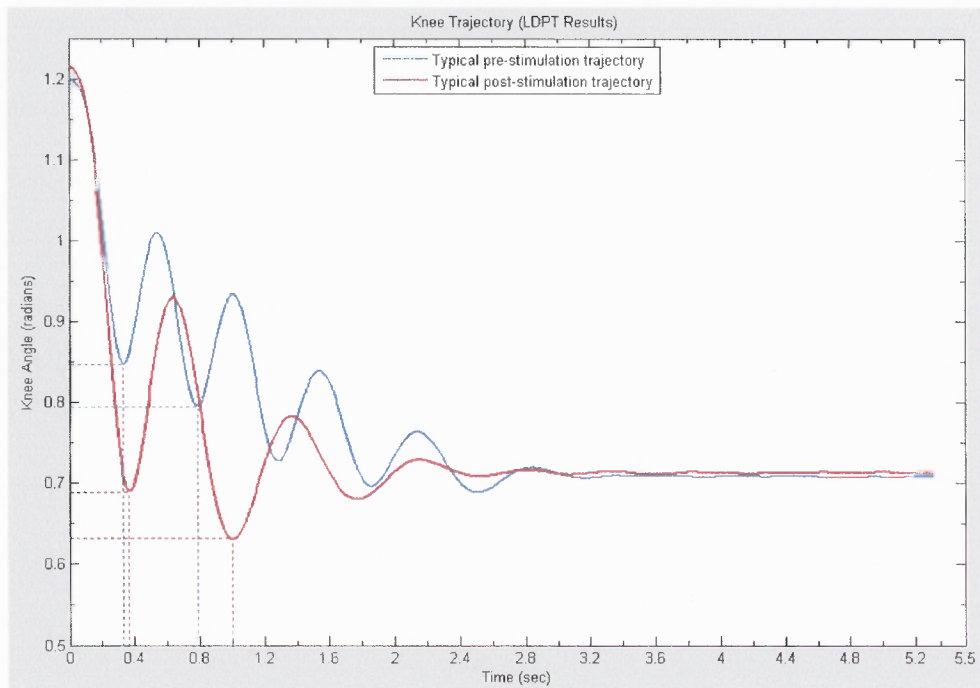


Figure 2.4 Knee trajectories collected during pre and post-stimulation LDPT for rotary otolith stimulation device.

2.2.2 Vertical, Linear Motion Stimulation

Based upon Fee's observation, he decided to investigate the effects of providing solely vertical stimulation to individuals with cerebral palsy. In order to conduct this study, it was necessary to develop a device to provide such stimulation, for which a vertical

motion platform was designed and built. During this study, ten individuals with cerebral palsy were subjected to fifteen minutes of vertical stimulation and the effects were quantified using the passive leg drop pendulum test. Figure 2.5 shows the LDPT results before and after stimulation. The position data before stimulation displays typical LDPT results from an individual with spastic cerebral palsy. The post-stimulation position data displays LDPT results more typical of a healthy individual without spasticity. The results suggest that the vertical stimulation caused an apparent reduction in leg muscle spasticity in the subject with cerebral palsy [1].

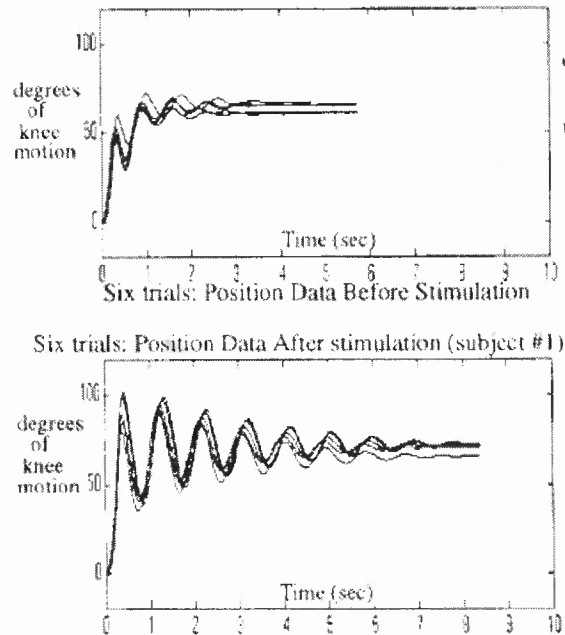


Figure 2.5 Leg drop pendulum test results showing effects of vertical, whole body stimulation of the otoliths. The top figure shows the position data before stimulation while the plot on the bottom displays the position data after stimulation. [1]

2.2.3 Important Experimental Testing Conditions

The goal of this thesis was to develop a device similar to the vertical motion platform developed for Fee's study [1]. This device is intended to be used for further exploration

of the effects of vertical, whole body stimulation of the otoliths. In order to do so, a number of factors needed to be carefully accounted for during the device design.

Research has shown the importance of proper timing of collecting data samples for exploring vestibular responses to various stimulations [18]. With regards to spaceflight, it is difficult to promptly obtain data upon immediately entering orbit due to the astronauts and cosmonauts being required to remove their space suits and prepare the testing apparatus. This delay allows for adaptation to microgravity to occur before collecting preflight data. Likewise, upon returning to Earth, a number of factors could contribute to compromising the test results. Many times, a large number of tests need to be conducted and each test may affect the results of the following tests. The crew members may intentionally move around prior to leaving the shuttle in an attempt to be able to walk off the shuttle or simply be physically exhausted and require rest before being able to be subjected to any tests [7]. Regardless of the reason, it has been shown that the inability to sample data immediately following spaceflight allows for postural readaptation to occur prior to actual data collection [18]. For the design of this device, it was important to account for this and make it possible to promptly collect data prior to and following stimulation of the saccule. Finally, a major advantage of spaceflight is that it allows for longer exposures to microgravity [7]. This allows for assurance of complete adaptation to microgravity. As stated earlier, this is difficult to achieve on Earth; but with the proper stimulation from a well designed device and test method, the skew between microgravity and simulated microgravity will ideally be minimized. The length of exposure to microgravity appears to play a role in the overall effect of the stimulation, and so the device needed to be designed to allow for extended durations of operation.

CHAPTER 3

DEVELOPMENT OF THE DEVICE

3.1 Product Design Specifications

Prior to designing the device intended to provide whole body stimulation of the otoliths, it was necessary to understand exactly what needed to be designed. Thus, formulating a list of design specifications was required to understand the requirements and goals that the device was intended to meet. Upon completion of the product design specifications, the device could then be designed within set guidelines. Listed below are the product design specifications that were formulated prior to the actual designing of the device.

1. Capable of achieving at least half of the acceleration due to gravity
2. Constrained for solely vertical motion
3. Capable of extended duration stimulation
4. Capable of achieving a measurable change in vertical position
5. Capable of testing adolescents
6. Capable of performing LDPT immediately prior to and after stimulation
7. Safe
8. Easily transportable
9. Compact
10. Aesthetically pleasing
11. Durable
12. Long life expectancy

In order to conduct research that will investigate the effects of whole body stimulation of the otoliths, the underlying mechanisms of the otolith organs needed to be

considered when designing the device. As stated earlier, when in an upright position, the saccule senses vertical accelerations. This is demonstrated when astronauts are subjected to microgravity conditions during spaceflight and develop muscle atrophy. From the study conducted using the rotary motion device, it was concluded that a motion with a vertical acceleration approximately half that of gravity caused a reduction in spasticity. Since the goal of this device is to provide stimulation that leads to a temporary reduction in spasticity, it was determined that the device needed to achieve at least half of the gravitational acceleration with the goal of mimicking microgravity by reaching full gravitational acceleration. Secondly, the device needed to be constrained to move only in the vertical direction. This is to only provide stimulation to the saccule, as the utricle is not of interest in this research.

Spaceflight typically takes place over a long time period and thus the length of exposure to microgravity conditions must be factored in when considering the effects of the stimulation on spasticity. Therefore, the device needed to be designed to be capable of providing extended durations of stimulation. As for the free-fall distance, it is unknown as to what is required to stimulate the saccule and therefore a conservatively long distance had to be incorporated into the design.

The optimal age group to be tested for this research had to be determined as well. Understanding that the LDPT requires the subject not to intervene requires some discipline on the part of the test subject. Also, it was concluded that the subjects were to be ambulatory. From these requirements, it was determined that adolescents would be the best subjects for studies to be conducted with this device. Therefore, it was necessary to design the device to be capable of performing in a usual manner when an adolescent

subject is on the device. As seen post spaceflight, subjects readapt to Earth's gravitational forces rather quickly and therefore this device needed to be capable of quickly conducting the LDPT immediately after the vestibular stimulation session. It was assumed that if this could be achieved, then it would be possible to conduct the LDPT immediately before the stimulation just as easily and timely.

After designing for the research to be conducted, it is also important to consider a variety of additional factors. The product design specifications listed above from numbers 7 through 12 are these additional factors that play a key role in a well designed device. Safety is a very important factor that was required to acknowledge considering testing was going to be conducted on human subjects. It was important to ensure that all precautions were taken to prevent injury. Also, the device most likely will be used in multiple venues over time and therefore had to be designed to be easily transportable. This included factoring in the device weight and size during its design phase. As with most things, an aesthetically pleasing final product was desired. This increases the comfort factor for the human subjects. Finally, the device needed to be durable. It is to be used indoors and typically in a clean environment, but as with all things, unexpected hardships had to be accounted for to ensure a long life expectancy of the device. The device components had to be chosen and designed to achieve the greatest length of life for the device.

3.2 Preliminary Design Calculations

Prior to designing the device, it was necessary to perform a variety of calculations in order to ensure the proper components were to be incorporated into the design. These calculations included determining the time for an object to fall a certain distance and the

force necessary to raise the same object the same distance in a specified amount of time. In order to perform these calculations, it was necessary to make a few assumptions. First, it was assumed that a four inch free-fall would be a reasonable change in distance to provide proper stimulation and so this value was decided upon for the design. Secondly, it was assumed that this device would be used with up to a 200 pound person, which allows for the device to be suitable for a wide range of adolescents. With these assumptions, the necessary calculations could be performed to determine the proper components to be used with the device.

3.2.1 Required Lifting Force

As stated earlier, it was assumed that this device was to be designed for use with up to a 200 pound person. In addition, a specially designed chair is used in conjunction with this device as an interface between the subject and the device. Upon weighing the chair, it was found to weigh approximately 60 pounds. In addition to this weight, a number of components of the device were assumed to possibly be required to be lifted as well during stimulation, of which was conservatively assumed to be approximately 15 pounds. All together, the device was to be capable of lifting a total of 275 pounds. Therefore, this value was used for calculating the maximum lifting force requirements. At this point it was understood that the total downward force of the sum of the person, chair, and device was equal to 275 lbf.

The fact that the device was intended to be capable of lifting a 275 lbf load narrows down the options as to which mechanism would be incorporated into the design to perform this function. Multiple options are available for such a task, including hydraulic, pneumatic, and electric actuators. However, electric actuators did not seem to

meet the force requirement and the use of hydraulics for such a task would be unclean for use in the required venues. On the other hand, pneumatic air cylinders provide large forces and are clean. Therefore, a pneumatic system was chosen as the driving mechanism for this device.

Table 3.1 shows the upward acceleration of a 275 lbf load over a range of input pressures for five pneumatic air cylinders with varying bore diameter. The negative values represent a downward acceleration and thus the load is incapable of being raised in those cases. From this table, it can be concluded that a single air cylinder with a bore diameter of 2 inches is the minimum size that is capable of lifting the maximum rated load. However, the 2 inch cylinder is on the borderline and with any unanticipated inertial forces or additional loads, it may prove to be unsuitable for the device. At the moment, it would appear that a 2.5 inch or 3 inch bore air cylinder would be suitable for the design.

Table 3.1 Upward Acceleration (ft/s^2) of a 275 lbf by a Single Pneumatic Air Cylinder

Input Pressure (psi)	Bore Size (In)				
	1.0625	1.5	2	2.5	3
10	-31.137	-30.107	-28.498	-26.431	-23.904
15	-30.618	-29.073	-26.661	-23.559	-19.769
20	-30.099	-28.039	-24.823	-20.688	-15.634
25	-29.581	-27.005	-22.985	-17.816	-11.499
30	-29.062	-25.972	-21.147	-14.945	-7.364
35	-28.543	-24.938	-19.310	-12.073	-3.229
40	-28.025	-23.904	-17.472	-9.202	0.906
45	-27.506	-22.870	-15.634	-6.330	5.041
50	-26.987	-21.837	-13.796	-3.459	9.176
55	-26.469	-20.803	-11.958	-0.587	13.311
60	-25.950	-19.769	-10.121	2.284	17.446
65	-25.431	-18.735	-8.283	5.156	21.581
70	-24.913	-17.702	-6.445	8.027	25.716
75	-24.394	-16.668	-4.607	10.899	29.851
80	-23.875	-15.634	-2.770	13.770	33.986
85	-23.357	-14.600	-0.932	16.642	38.121
90	-22.838	-13.567	0.906	19.513	42.256

3.2.2 Time for Free-Fall

In order to optimize the performance of the device, it was necessary to design for the extreme cases. The maximum free-fall that this device was assumed to achieve was four inches. Therefore, calculations were performed to determine the length of time it takes for an object to fall four inches. In order to do so, all external forces, such as air resistance, were neglected. Equations 3.1 and 3.2, below, represent the equations of motion used during these calculations.

$$v = v_0 + a\Delta t \quad (3.1)$$

$$v^2 = v_0^2 + 2a\Delta s \quad (3.2)$$

In these equations, v and v_0 represent the final and initial velocities of the body, respectively, while a is the constant acceleration of the body, or in this case, gravity. Finally, Δt and Δs are the changes in time and position between two instances in time. From these two equations and neglecting inertial forces, it was determined that it would take an object approximately 0.144 seconds to free-fall four inches.

Air cylinders have an orifice in which air can be expelled from with a much larger inner bore diameter. The larger the cylinder bore, the larger the volume of air that needs to be expelled from the orifice in the same amount of time. Table 3.2 shows the air expulsion rates in standard cubic feet per minute (SCFM) for achievement of free-fall. The goal is to minimize the difference between this theoretical air expulsion rate and the actual air expulsion rate of the device. From Table 3.2, it can be concluded that a

cylinder with a smaller bore has considerably less air to be expelled than a cylinder with a larger bore.

Table 3.2 Air Expulsion Rate (SCFM) from an Air Cylinder for a Four Inch Free-Fall

Stroke Length (in)	Bore Size (in)				
	1.0625	1.5	2	2.5	3
4	0.855	1.705	3.031	4.736	6.820

3.2.3 Choosing a Pneumatic Air Cylinder

Upon comparison of the air expulsion rates and the lifting capabilities of the five actuator sizes, it was concluded that a pneumatic air cylinder with a 1.5 inch bore would provide optimal performance. However the design specifications could not be met with a single actuator. Four 1.5 inch bore pneumatic air cylinders can provide the lifting force of a single 3 inch bore air cylinder, but allow the theoretical air expulsion rate to be a value of 1.705 SCFM, which is 1/4th that of the 3 inch bore cylinder. Table 3.3 shows the upward acceleration due to the lifting force of four actuators designed in parallel. Four 1.5 inch bore air cylinders are capable of lifting a 275 lbf load at a pressure of 40 psi. The smallest cylinder can achieve the same results at a pressure of 80 psi, but this is unacceptable for this design. From this, it was determined that the design was to incorporate four 1.5 inch bore pneumatic air cylinders in parallel.

Table 3.3 Upward Acceleration (ft/s^2) of a 275 lbf by Four Pneumatic Air Cylinders

Input Pressure (psi)	Bore Size (in)				
	1.0625	1.5	2	2.5	3
10	-28.025	-23.904	-17.472	-9.202	0.906
15	-25.950	-19.769	-10.121	2.284	17.446
20	-23.875	-15.634	-2.770	13.770	33.986
25	-21.801	-11.499	4.581	25.256	50.526
30	-19.726	-7.364	11.933	36.743	67.066
35	-17.651	-3.229	19.284	48.229	83.606
40	-15.577	0.906	26.635	59.715	100.146
45	-13.502	5.041	33.986	71.201	116.686
50	-11.427	9.176	41.337	82.687	133.226
55	-9.353	13.311	48.688	94.173	149.766
60	-7.278	17.446	56.039	105.659	166.306
65	-5.203	21.581	63.390	117.145	182.846
70	-3.129	25.716	70.741	128.631	199.386
75	-1.054	29.851	78.092	140.117	215.926
80	1.021	33.986	85.444	151.603	232.466
85	3.095	38.121	92.795	163.090	249.006
90	5.170	42.256	100.146	174.576	265.545

3.2.4 Air Compressor Requirements

An air compressor is capable of compressing air at a specified rate. For this design, the production rate needed to be greater than the volumetric rate of air consumption by the system. In order to determine the maximum possible volumetric rate of air consumption by the device, it was assumed that the device was to be operated without a human subject and therefore only would be required to lift a 75 lbf load. The maximum pressure used for these calculations was 90 psi. It should be noted that this was also an assumption as the maximum operating pressure was yet to be known at this point in time. Using Equations 3.1 and 3.2, as defined earlier, the upward time duration would be a minimum of 0.182 seconds. As stated earlier, the free-fall duration would be 0.144 seconds for a four inch free-fall. With the assumption that there is no delay during operation of the

device, a single cycle would span 0.326 seconds, thus resulting in approximately 184 cycles per minute. Following further calculations, it was concluded that approximately 3 SCFM of air is required to operate the four cylinders continuously. Therefore, any compressor that is capable of compressing air at that rate is suitable for this application.

3.3 Technical Product Specifications

Earlier, the design specifications for this device were presented in detail. From that list of requirements, many decisions were made with regards to the design of the device in order to meet the formulated specifications. Appendices A through G provide specifications for many of the various components that are a part of this design.

Since a great deal of weight is to be raised and allowed to free-fall, it was understood that two main assemblies were necessary to be designed to allow for this to safely occur. First, a rigid and sturdy base frame would serve as the foundation of the device. Secondly, a mobile, yet rigid, frame for allowing for the vertical movements. Figure 3.1, below, shows the final assembly of the otolith stimulation platform base frame, consisting of anodized t-slotted aluminum extrusions joined with various anodized aluminum joining plates. Leveling feet were added to accommodate for unlevelled floors. Anodized aluminum was chosen due to its excellent resistance to corrosion, high strength, and low weight characteristics. The overall weight of the base frame was approximately 50 pounds. This is light enough to allow for the device to be easily transported. However, it is also heavy enough to keep the device from rocking or sliding along the floor during operation. The overall dimensions of the base frame are 24 inches on each side and 13 inches tall. The platform was designed to these dimensions to keep the lowest center of gravity possible and maintain a small, compact design. Finally, the

anodized aluminum is very aesthetically pleasing, a very important characteristic that helps to make a person comfortable enough to use the device even when they do not really know how well the device actually functions.

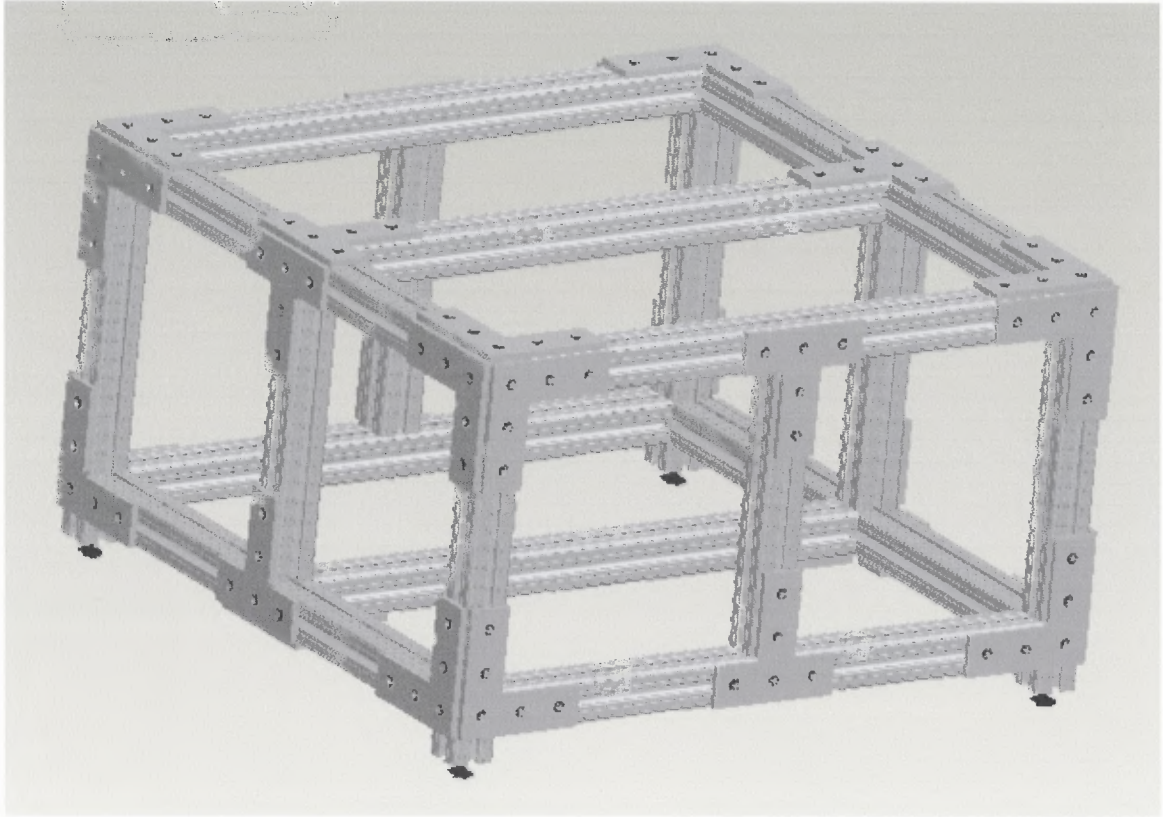


Figure 3.1 Otolith stimulation platform base.

As seen in Figure 3.1, the base was designed with vertical midline supports on each side to lower the amount of deflection that would occur on the horizontal t-slotted extrusions. This served to increase the overall rigidity of the frame. High rigidity proved to be a very important factor to prevent the pneumatic air cylinder piston from being allowed to deflect, which would result in its binding. In order to prevent this binding, the mobile frame was necessary to be highly rigid as well. Therefore, it was designed with 1.5" X 3" anodized, extruded aluminum tube as can be seen in Figure 3.2. The aluminum channel is robust and any deflection that may occur is small enough as to not cause the

pneumatic air cylinder pistons to deflect and bind. Part drawings for the anodized aluminum tubes can be viewed in Appendix G.

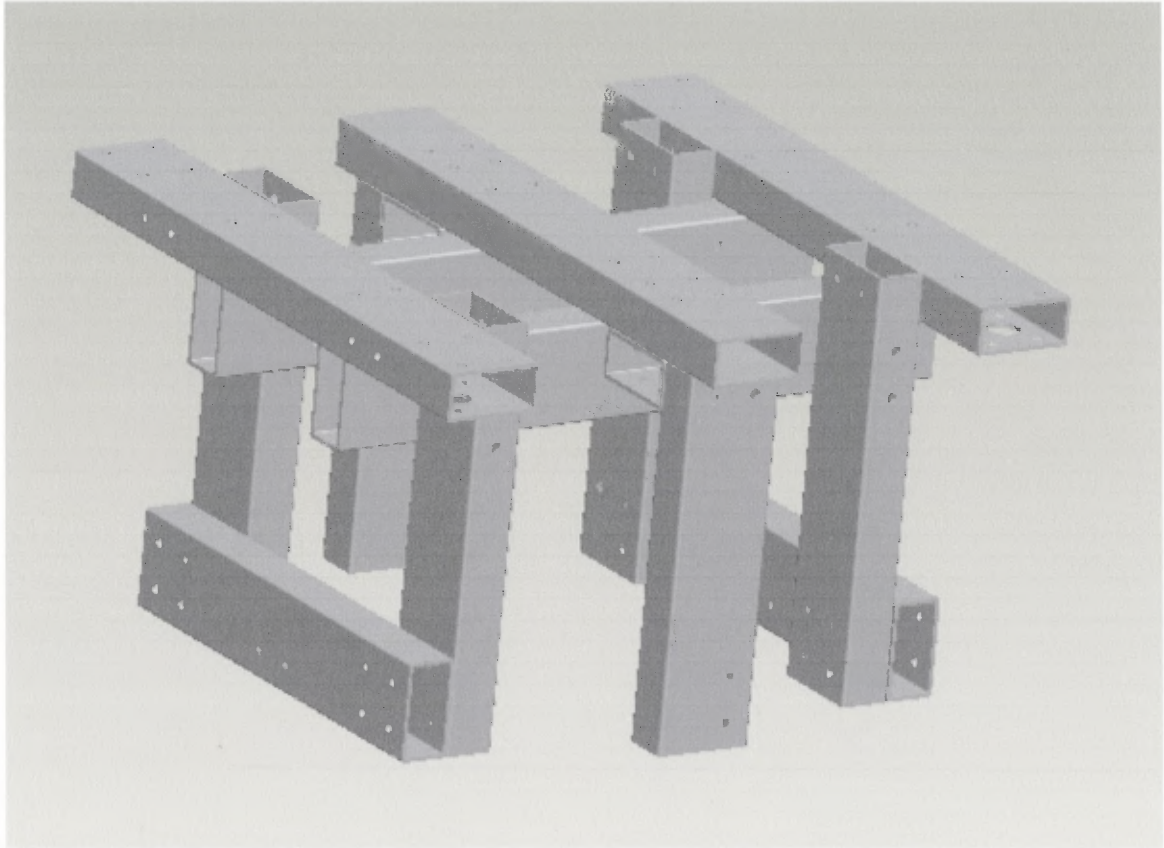


Figure 3.2 Otolith stimulation platform mobile frame.

As stated earlier, the main reason for developing this platform device was for providing whole body stimulation of the otoliths. Therefore, the main goal was to achieve free-fall motion. Without designing for free-fall, the device would be incapable of simulating microgravity and so in order to meet that requirement, low friction components are necessary and the motion needs to be constrained solely in the vertical direction. To achieve this goal, precision guide blocks and rails were incorporated into the device. These guide blocks and rails constrain the device to move vertically, thus preventing the actuator pistons from being able to bind. It is important that when

incorporating these components in parallel in the design that they are in fact actually parallel and vertical, as any variance from vertical will lead to friction and binding of the components. Figure 3.3 shows the base frame with the guide blocks (black) and rails (grey) on each side, in addition to the air cylinders near the corners. The rails are attached to the base frame, while the guide blocks attach to the mobile frame shown in Figure 3.2 and are able to move up and down the respective rails.

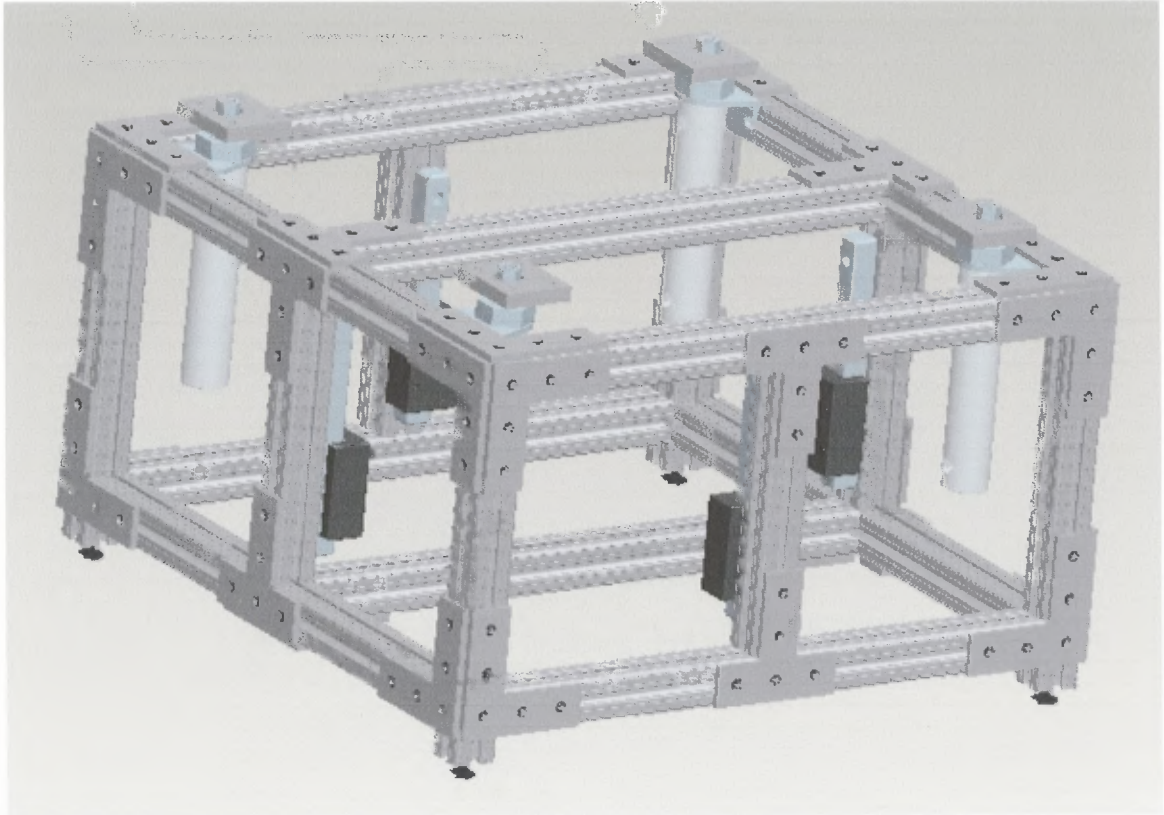


Figure 3.3 Otolith stimulation base frame with guide blocks, rails, and actuators.

In order to measure the friction caused by the guide blocks and rails, the pneumatic actuators were detached from the platform frame and the air hoses were removed from the actuators. This allowed the actuators to move with the mobile frame. The device, along with the chair, was then raised to its maximum height and allowed to free-fall. Figure 3.4 shows the results obtained using a three-dimensional camera motion

capture system. Shown in the position plots is that the device accelerates downward for four inches before it begins to decelerate. Of great importance here is the fact that the device achieves acceleration near to that of Earth's gravitational acceleration. This proves that minimal friction is induced into the system from the guide blocks and rails.

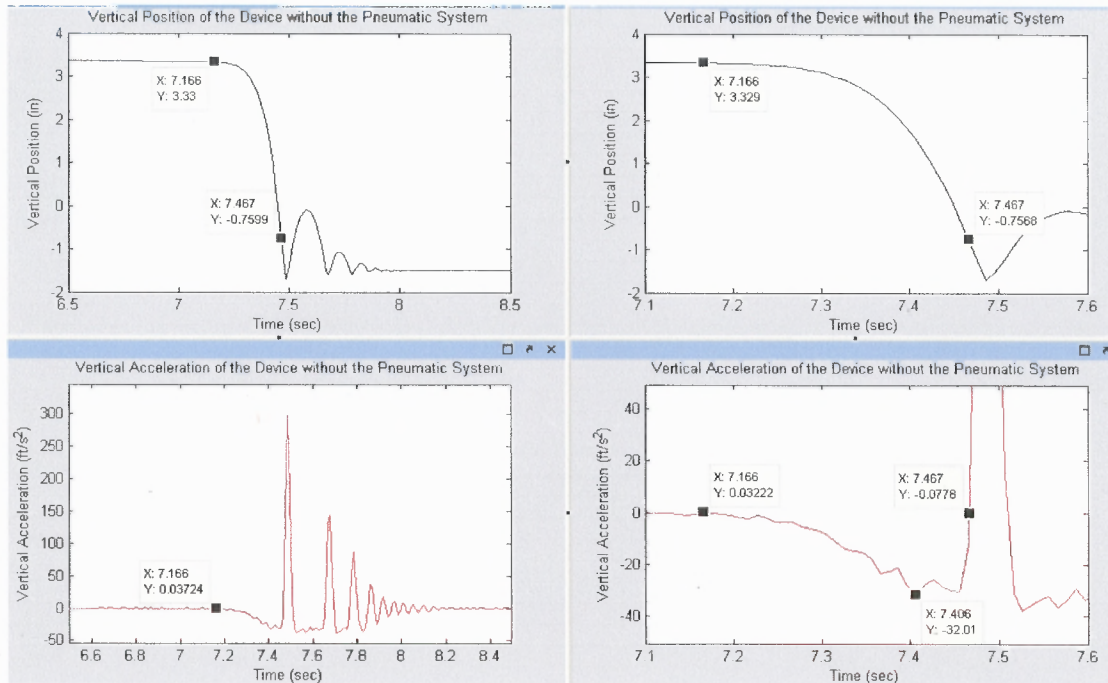
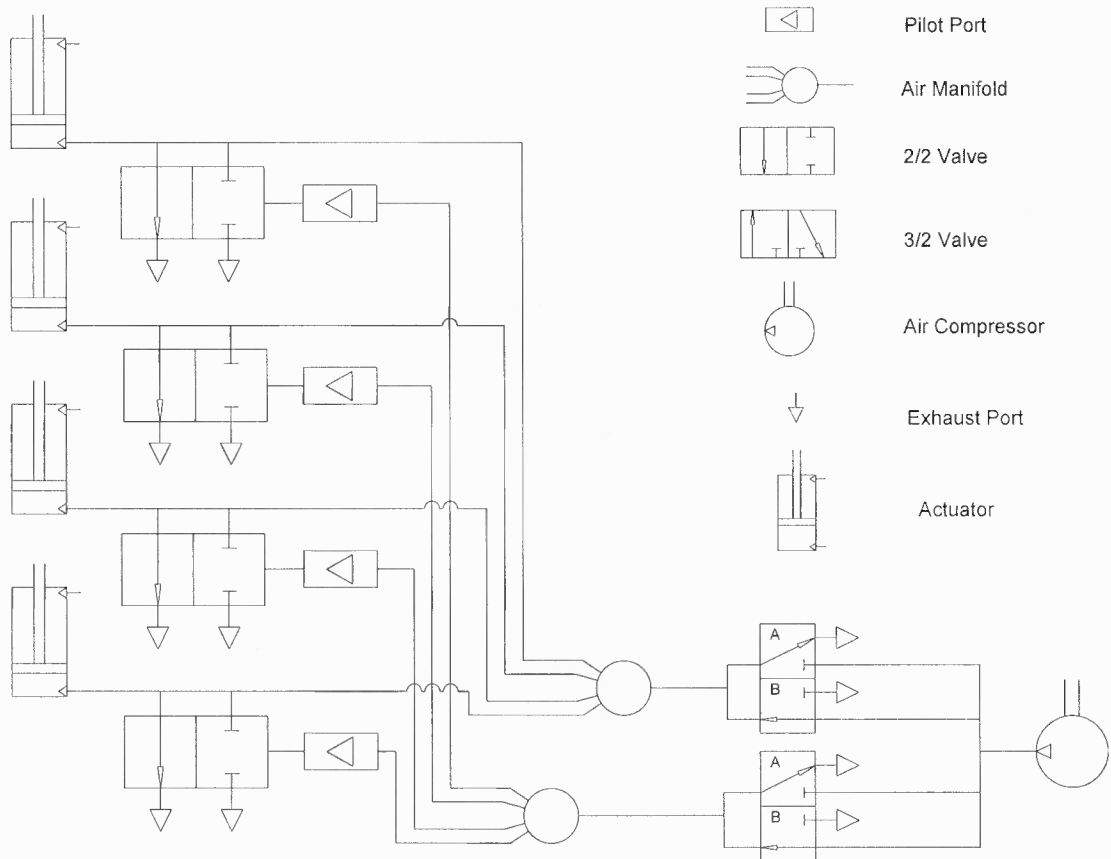


Figure 3.4 Position and acceleration data collected for stimulation platform without pneumatic system attached.

In addition to frictionless components, control valves were placed at the lower outlet port of the pneumatic actuator in order to provide an unrestricted exhaust port for the air in the cylinders to be expelled to the atmosphere during free-fall. While air is input into the actuators to raise the pistons, the control valves are shut off as to not allow air to flow in or out, thus ensuring the air is solely working to raise the pistons. No air is input into the upper actuator port during free-fall. Figure 3.5 depicts the pneumatic control system of the otolith stimulation device. In order to raise the actuator pistons, the upper solenoid adjacent to the compressor is signaled to open while the lower solenoid

adjacent to the compressor remains closed. To signal for the pistons and the device to free-fall, the upper solenoid is closed and the lower solenoid is opened, which provides air to the pilot ports of the control valves at the lower actuator outlets. This in turn opens the control valve to the atmosphere and allows for a brief period of free-fall.



*Note: The 2/2 valves depicted here are actually 3/2 normally open valves with the inlet plugged. They therefore function like 2/2 valves, hence the reason for being depicted as so in this schematic.

Figure 3.5 Pneumatic system schematic.

The pneumatic control system is controlled in part by the electrical control system of the otolith stimulation device, as shown in Figure 3.6. Due to component specifications, 8 VDC are applied to two reed relays. Reed relays were chosen for this application due to their rapid switching speeds and low cost. Initially, the relay has an

open circuit. When a digital output signal is generated from the laptop, a current is applied to the internal solenoid of the reed relay, thus causing the switch to close. This allows for current to pass to the control valves. At this point the control valves switch internal positions and air is allowed to flow through the control valves. The triggering of the relays can be performed individually using MATLAB. This can be seen in the program available in Appendix H.

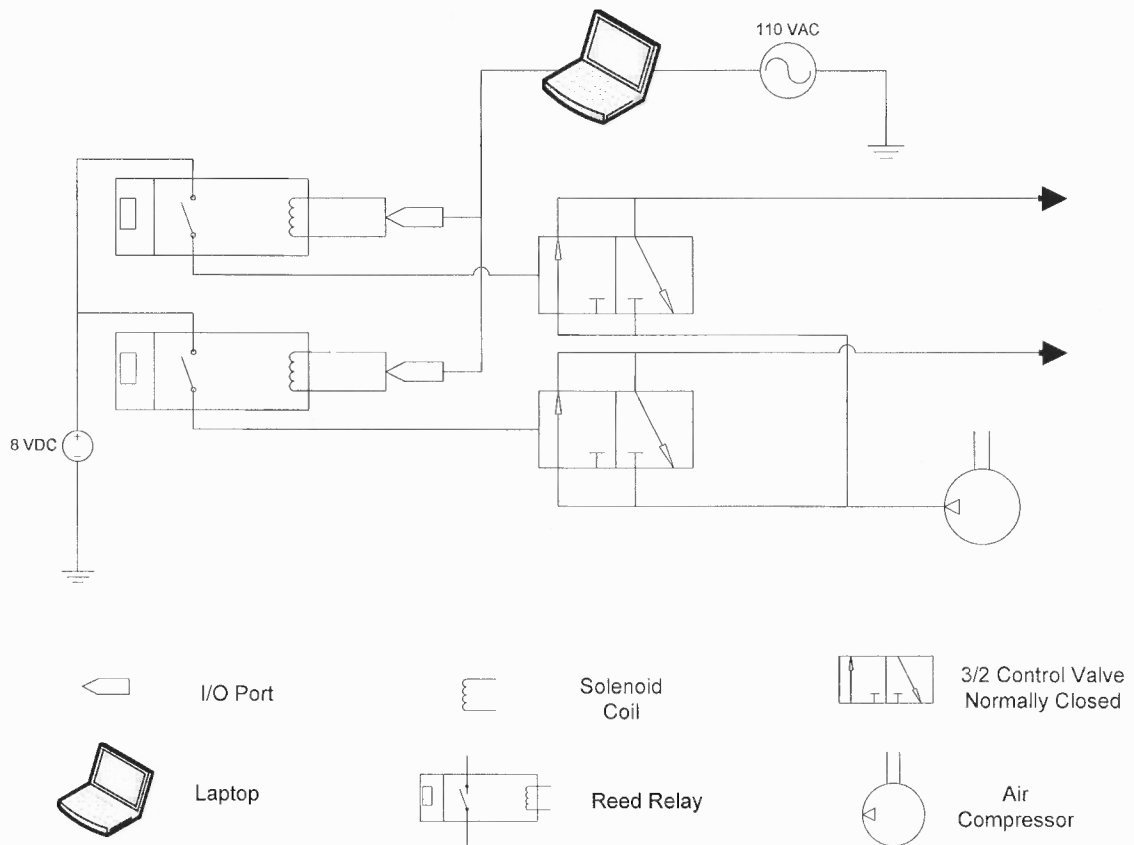


Figure 3.6 Electrical system diagram.

In addition to the electrical system diagram shown above, Figures 3.7 and 3.8 are snapshots of the breadboard, which contains the reed relays. The colored wires shown in these figures connect to the connection block shown in Figures 3.9 and 3.10. The close

up of the individual ports shows the wires connected to the first two digital input/output lines. Appendix C contains additional information regarding the connection block.

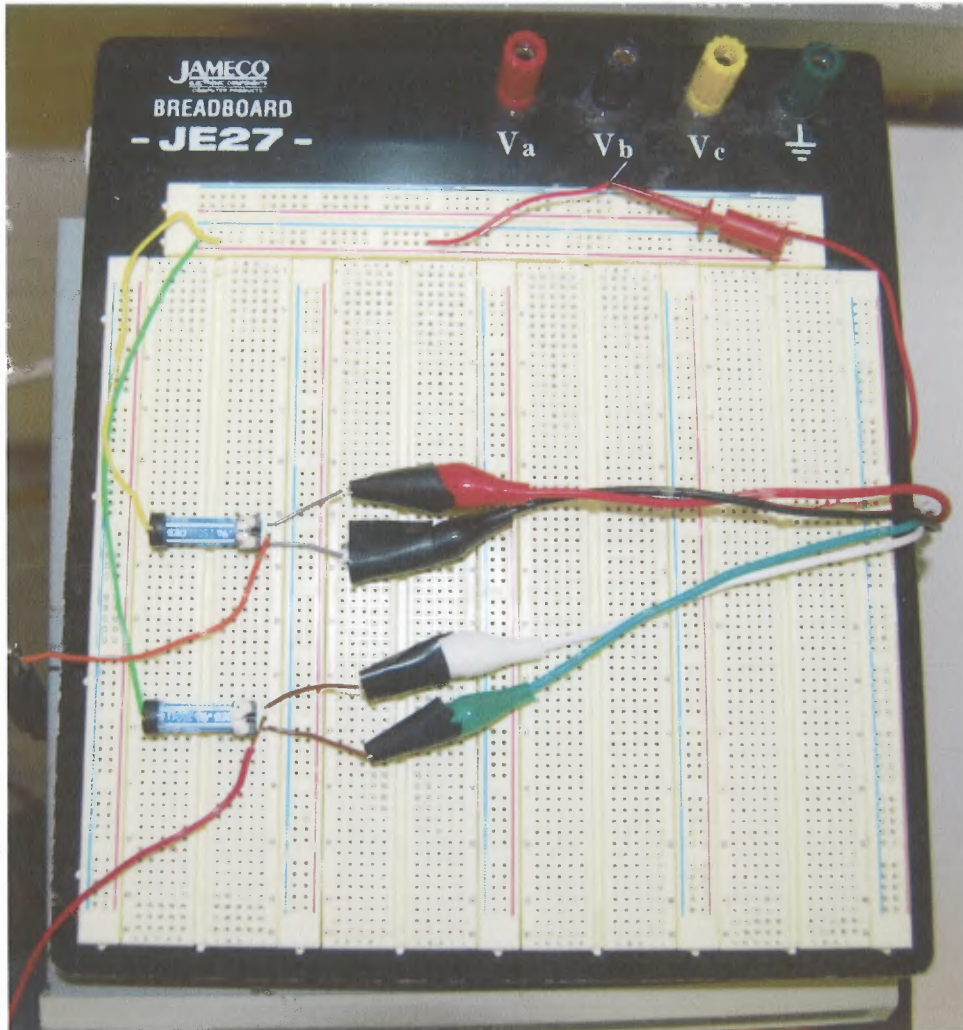


Figure 3.7 Breadboard with reed relays.

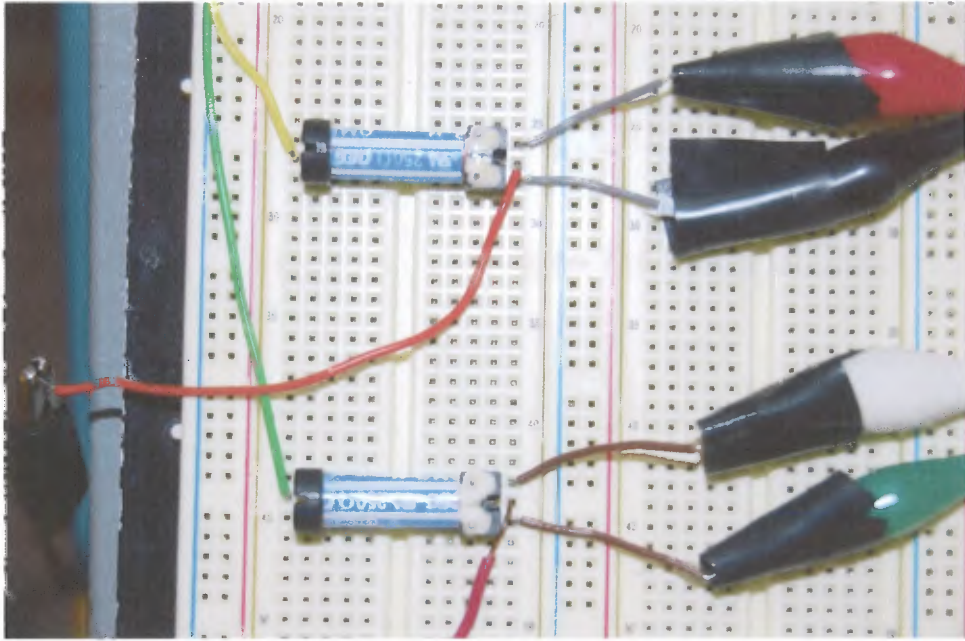


Figure 3.8 Close-up of relay connections.

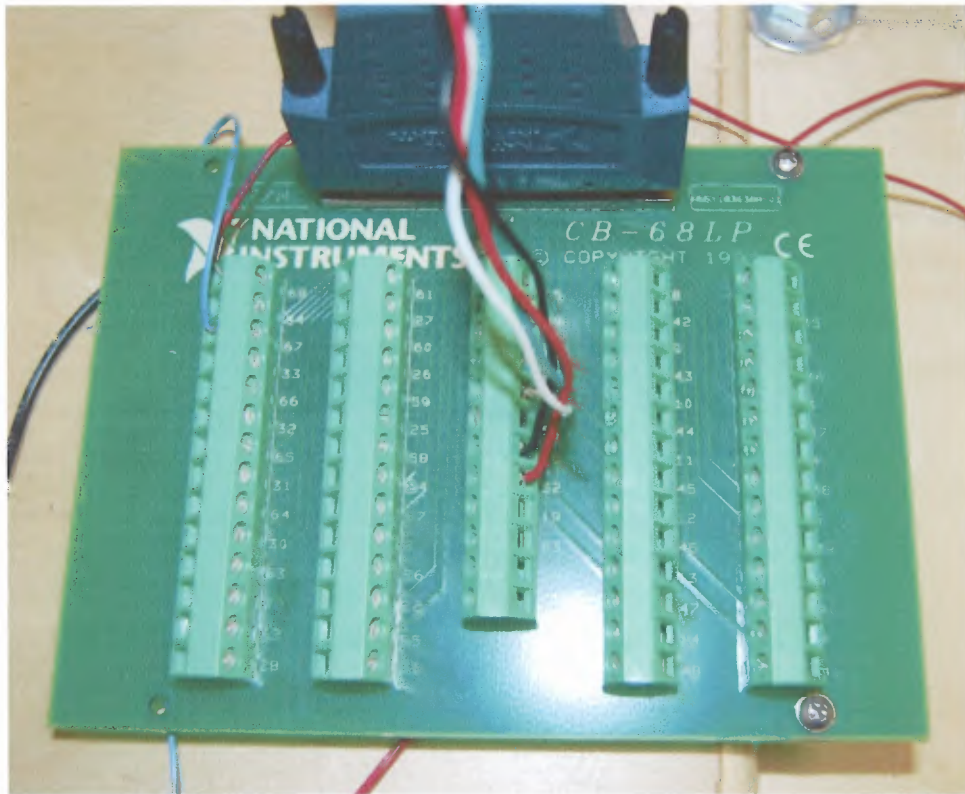


Figure 3.9 CB-68LP connection block.

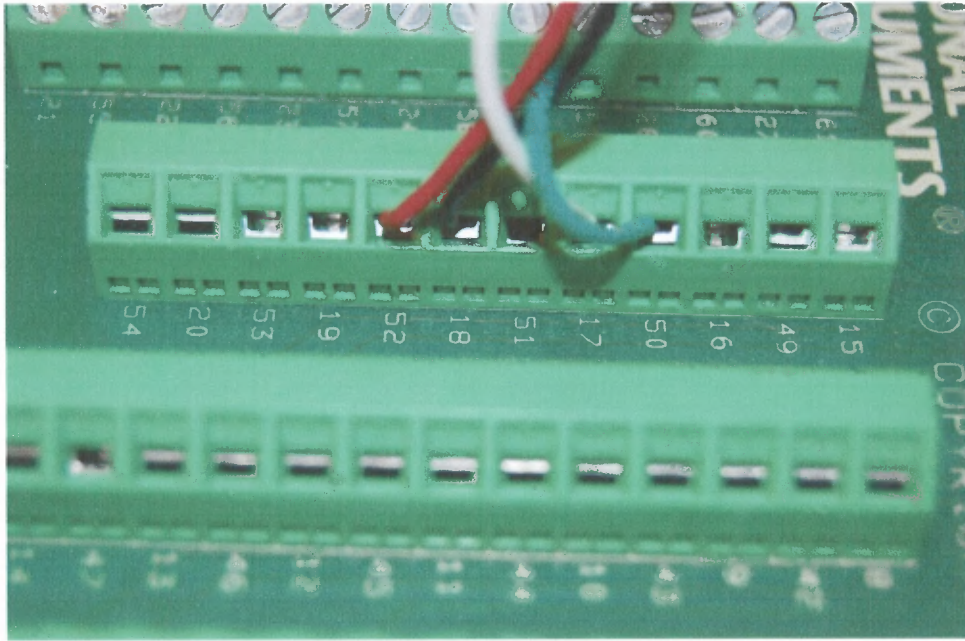


Figure 3.10 Close-up of DIO0 and DIO1 connection block ports.

Another design specification was that the device needed to be capable of achieving a measurable change in vertical position. This was achieved by incorporating a pneumatic air cylinder with a four inch stroke into the design at the corners of the base frame. The air cylinders were mounted to the frame as shown in Figure 3.3 above, while the piston mounting brackets (shown in Figure 3.3 and drawn in Appendix G) joined the actuator pistons to the mobile frame. The final assembly in its lowered state can be viewed in Figure 3.11, shown below. The final assembly in its raised state can be viewed in Figure 3.12. The device shown in Figure 3.12 is raised to its maximum height of four inches.

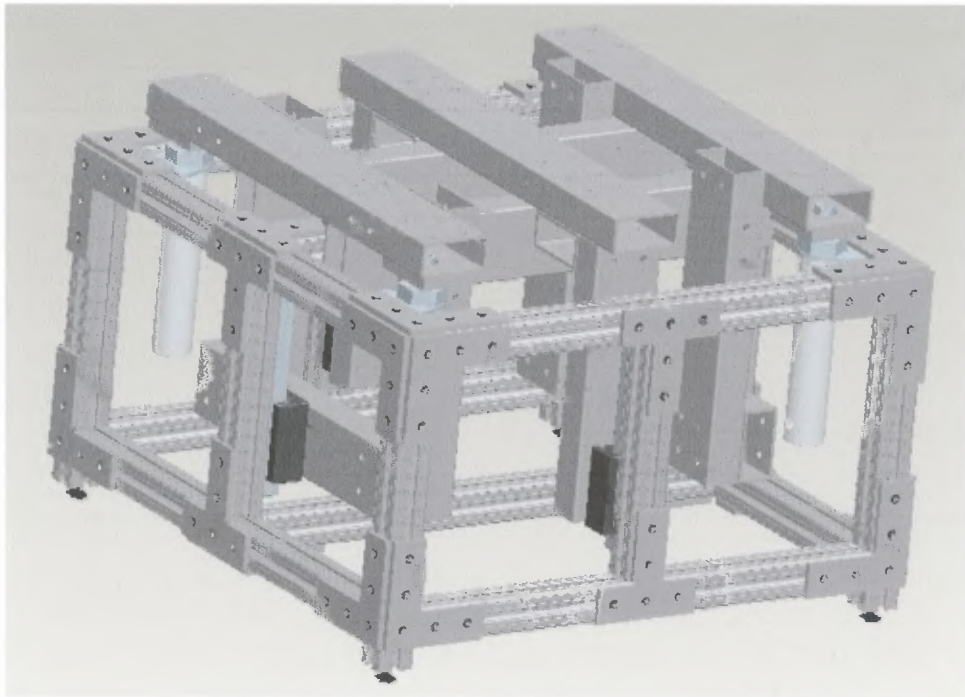


Figure 3.11 Final lowered assembly model.

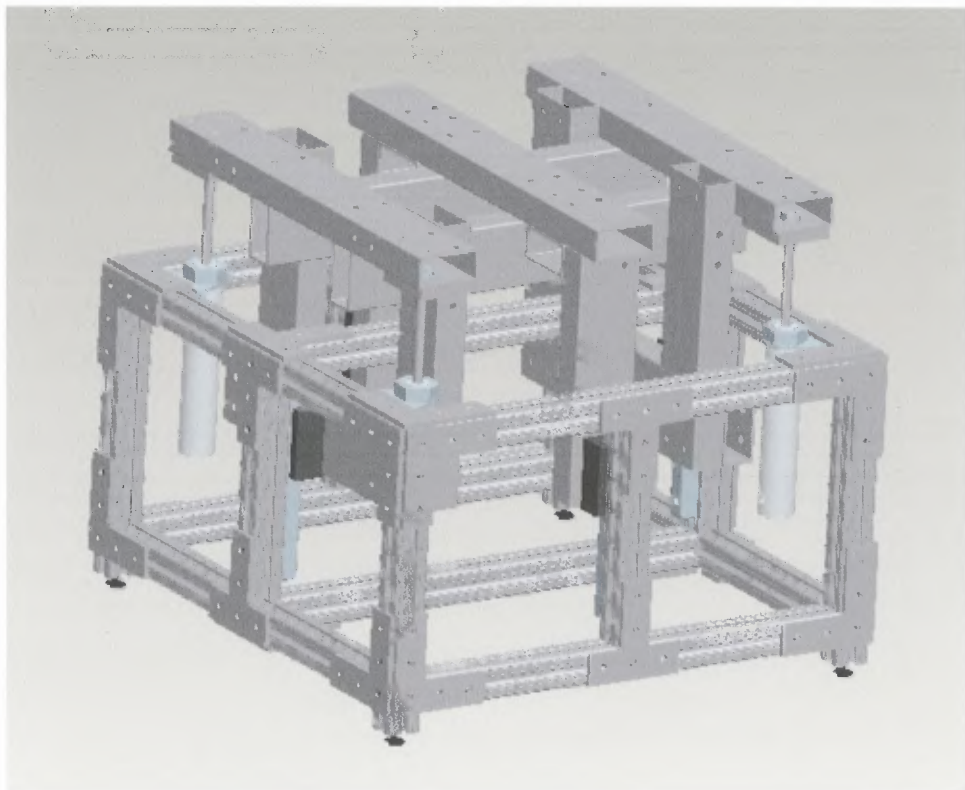


Figure 3.12 Final raised assembly model.

Figures 3.13 and 3.14 are snapshots of the actual device in its lowered and raised positions, respectively. In Figure 3.13, the system is at rest, hence the device being lowered. On the other hand, in Figure 3.14, compressed air is forcing the device into the raised position, during which the system is waiting on the signal that eventually results in the device to descend back down towards its resting position.



Figure 3.13 Final device in lowered position.

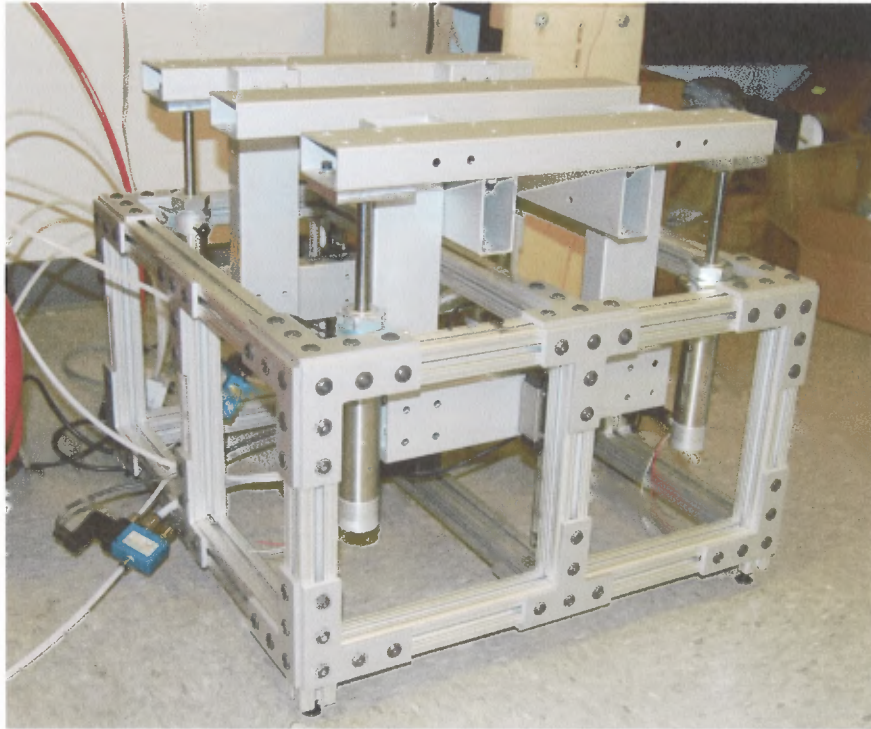


Figure 3.14 Final device in raised position.

From the preliminary calculations computed prior to designing the otolith stimulation platform, it was determined that the device would require an air source capable of providing a maximum of 3 SCFM of air to the system. A single air compressor, described in Appendix F, is suitable for meeting this specification. With this compressor, continual operation of the device is possible, thus allowing for the device to be capable of extended duration stimulation.

As described largely in the literature, it is important to conduct the LDPT immediately following microgravity otolith stimulation. This device allows for this in a number of ways. First, a chair allowing the LDPT to be conducted easily can be used with this device. Figure 3.15 shows a picture of this chair on the stimulation platform. The chair is attached to the mobile frame via the access holes that were machined for joining the mobile frame aluminum tube components. The chair is rather large and so it

was important not to increase the overall height any more than necessary. The device itself was designed with that in mind and so it is relatively small compared to the chair. The person conducting the LDPT can easily perform the test when the platform is lowered. The device is designed to settle to its lowered level upon completion of its operation and therefore the LDPT can be performed immediately following stimulation.

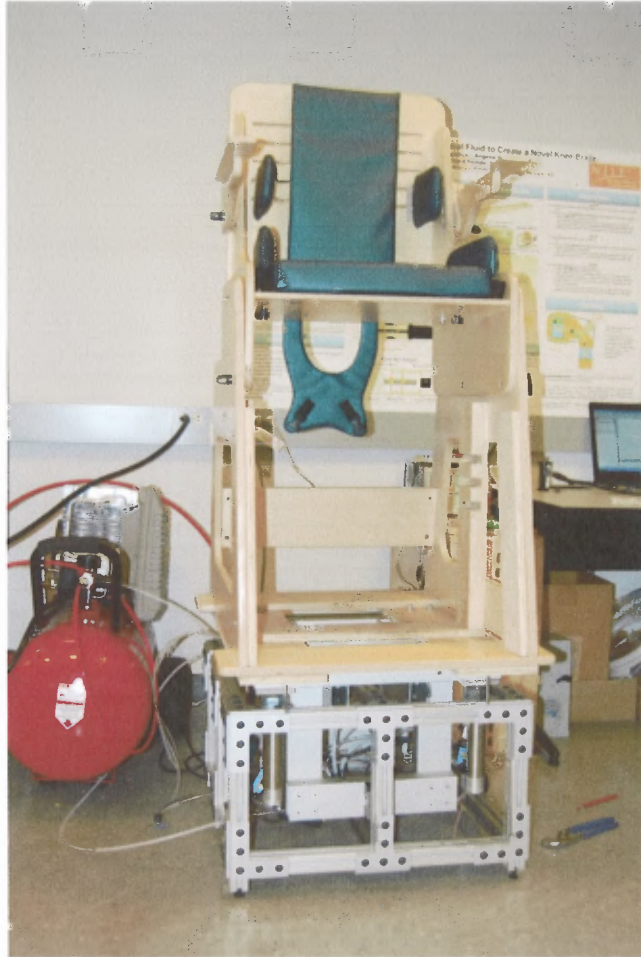


Figure 3.15 Otolith stimulation platform with chair designed for LDPT.

CHAPTER 4

DEVICE PERFORMANCE RESULTS

As stated earlier, the age group that this device is intended for is adolescents. It was assumed that if the device was found to function correctly when a 200 pound person was being tested, then the device would be suitable for testing most adolescents. To test the capability of the device, a 180 pound person was subjected to 60 seconds of stimulation and the position, velocity, and acceleration were computed from voltage data collected from the analog signal generated from a single position feedback cylinder. Figure 4.1 is a picture of the setup of the device with the 180 pound person sitting in the chair. Figure 4.2 shows the position, velocity, and acceleration of the device for a 180 pound person. It should be noted that the mobile frame weighs approximately 35 pounds and the chair weighs approximately 60 pounds. The system air pressure was set to 75 psi.



Figure 4.1 180 pound person sitting in chair attached to device following stimulation.

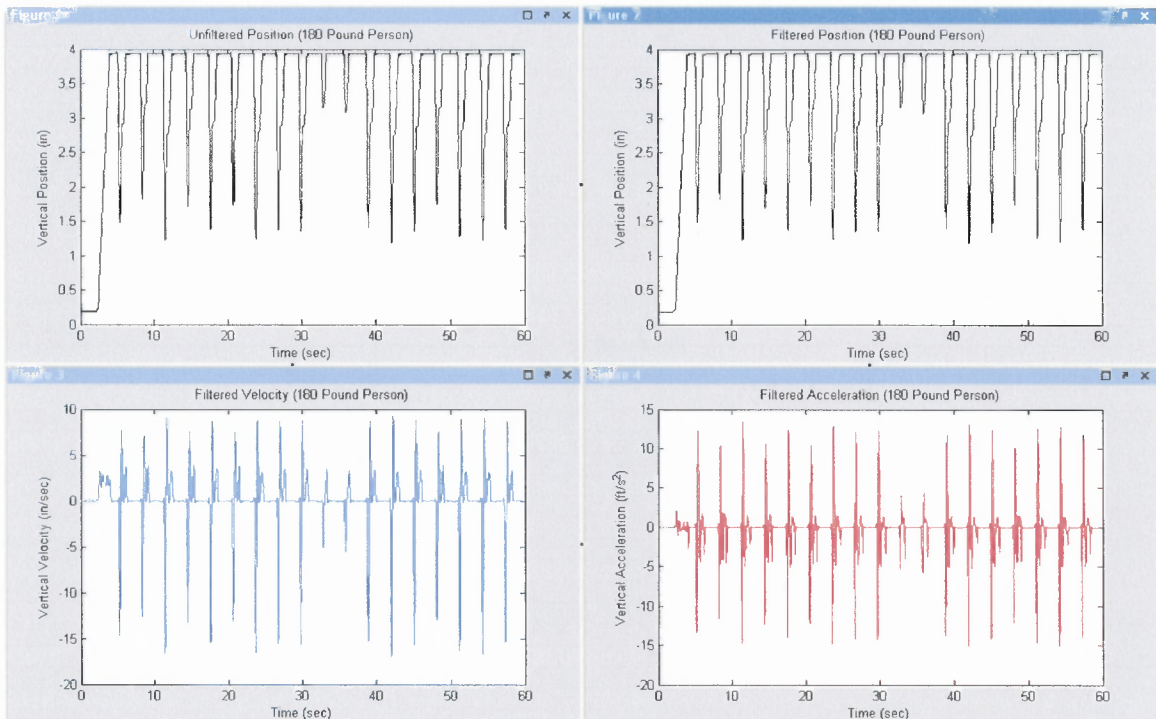


Figure 4.2 Position, velocity, and acceleration data collected for a 180 pound person.

For the data presented in Figure 4.2, the position data was filtered at 6 Hertz using a fourth order butterworth filter. The program that was run during this test can be viewed in Appendix H. From the position data, it can be noticed that the device typically fell between two and three inches before rising.

Regardless of weight, the device was found to achieve approximately half of the gravitational acceleration on Earth. The plot of the acceleration data confirms this for a 180 pound person. The goal was to approach gravity. This difference is most likely due to a number of factors. First of all, although the components are theoretically frictionless, they most likely are not actually completely frictionless. Secondly, the pneumatic system is difficult to control as air compresses, which must be accounted for during the free-fall stage. Air must be applied upward to slow the device during its descent. This prevents the device from being in total free-fall.

Figures 4.3 and 4.4 show sixty seconds of data collected during operation of the device for two separate loading scenarios. In Figure 4.3, a 90 pound load was added to the system and the air pressure was adjusted to 60 psi. Figure 4.5 shows the setup with the additional weight. In Figure 4.4, no additional load was added to the device and the air pressure was adjusted to 40 psi. Figure 4.6 shows the setup without any additional weight added to the system. The programs run to collect the data presented in Figures 4.3 and 4.4 are also provided in Appendix H.

Upon inspection of Figures 4.3 and 4.4, it can be concluded that the device performance for each case is closely similar to one another. Likewise, they are both similar to the 180 pound loading scenario. Once again, a two to three inch drop is visible, while the acceleration hovers around half of the acceleration due to Earth's gravity.

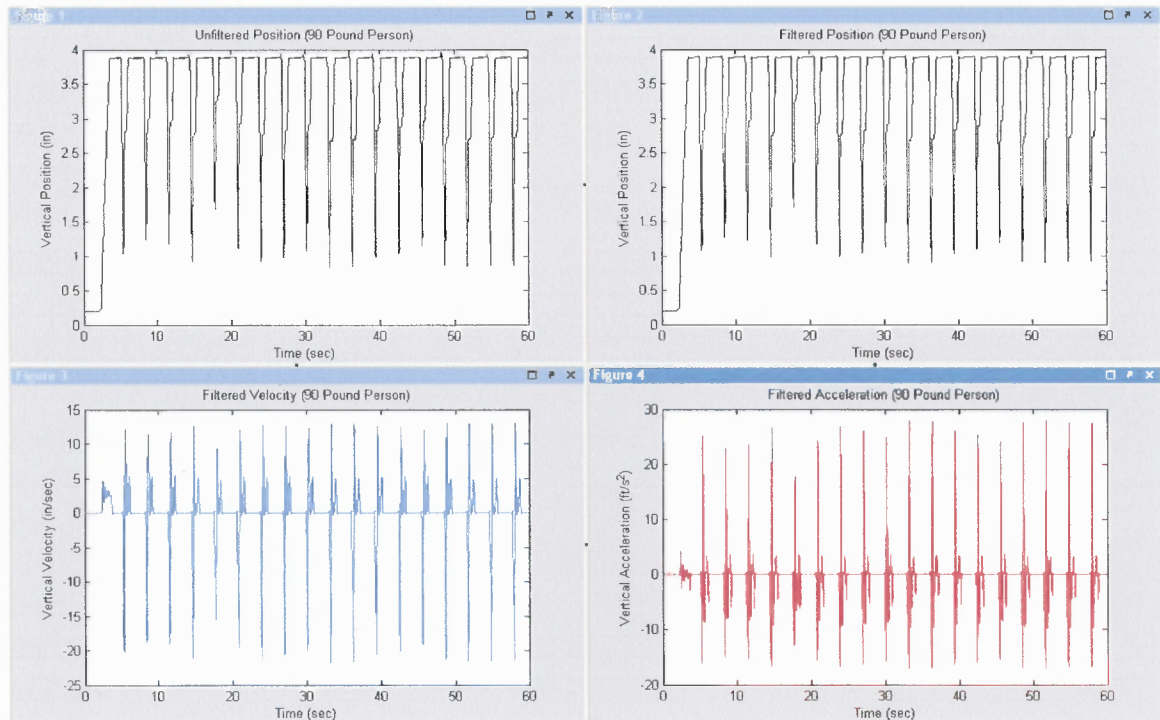


Figure 4.3 Position, velocity, and acceleration data collected for a 90 pound person.

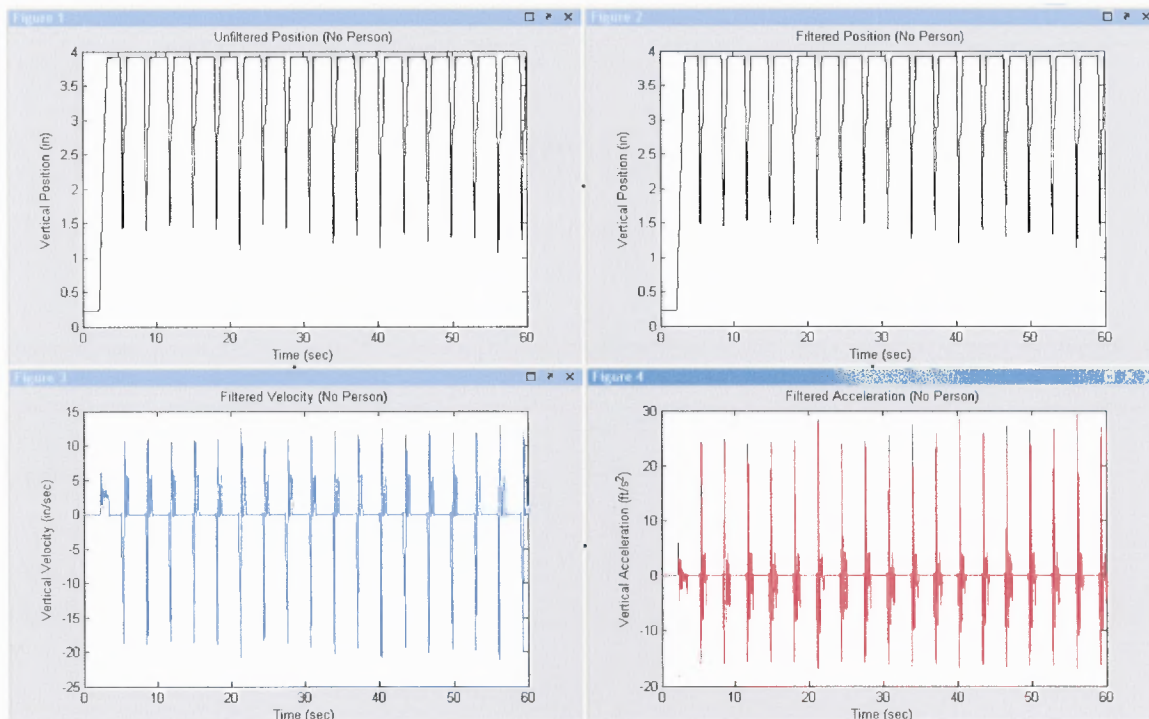


Figure 4.4 Position, velocity, and acceleration data collected for zero load.

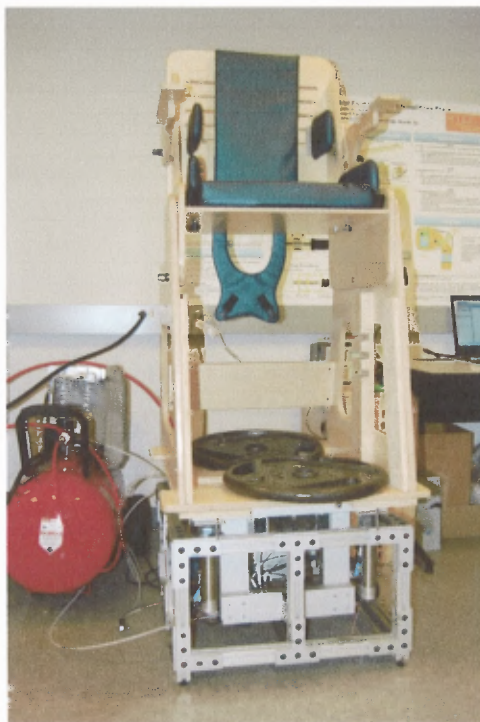


Figure 4.5 90 pound load added to otolith stimulation device.



Figure 4.6 Otolith stimulation device with no additional loading.

Figures 4.7 and 4.8 show two periods of the data collected without loading. The device achieves its maximum downward acceleration approximately 100 milliseconds after it begins falling. It reaches its maximum downward velocity approximately 150 milliseconds after it begins falling. Due to the delayed response time of the control valves, there is an approximate 50 millisecond delay in the system. Therefore, for the zero loading case, the free-fall is triggered to begin 50 milliseconds prior to its actual initial descent. Additionally, 150 milliseconds after the free-fall trigger occurs, the trigger to raise the device takes place. This corresponds to 100 milliseconds after the initial descent, which is also the point at which the downward acceleration is the greatest. Once again, due to the control valve response delay, the upward air pressure is not applied for another 50 milliseconds, which corresponds to approximately 150 milliseconds after the initial descent. As stated earlier, this is the point at which the

downward velocity is greatest. With an upward air pressure now being applied at this point in time, the device begins to slow down as the air in the system compresses until the device slows to a halt and reverses its direction upward. While rising, the human/device briefly settled before rising again. This is due to the overshoot from the descent as the air compresses. The amount of force at that point to raise the device is the combination of the force from the air input and the force from the compressed air (similar to a spring force). This causes the system to overshoot while rising and when the air “catches up” with the device, it smoothly ascends to the peak. Overall, this is a con of using a pneumatic system as it is difficult to control.

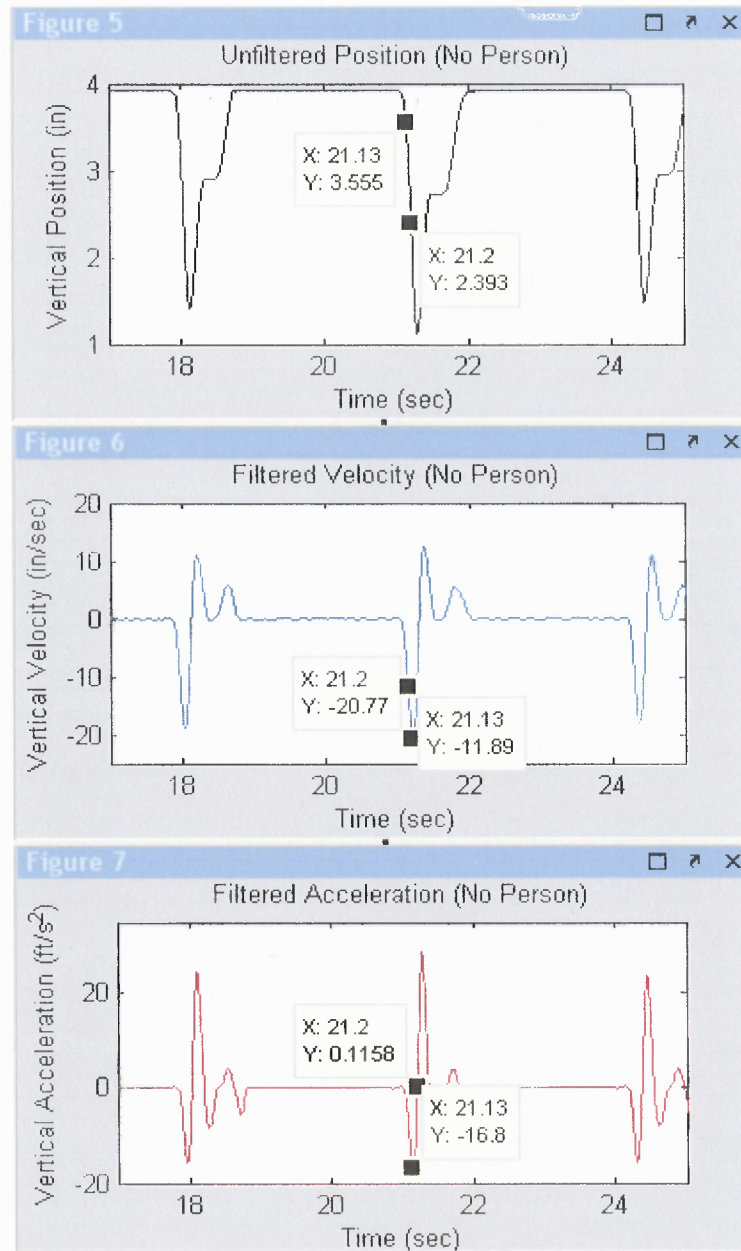


Figure 4.7 Portion of position, velocity, and acceleration data collected for zero load.

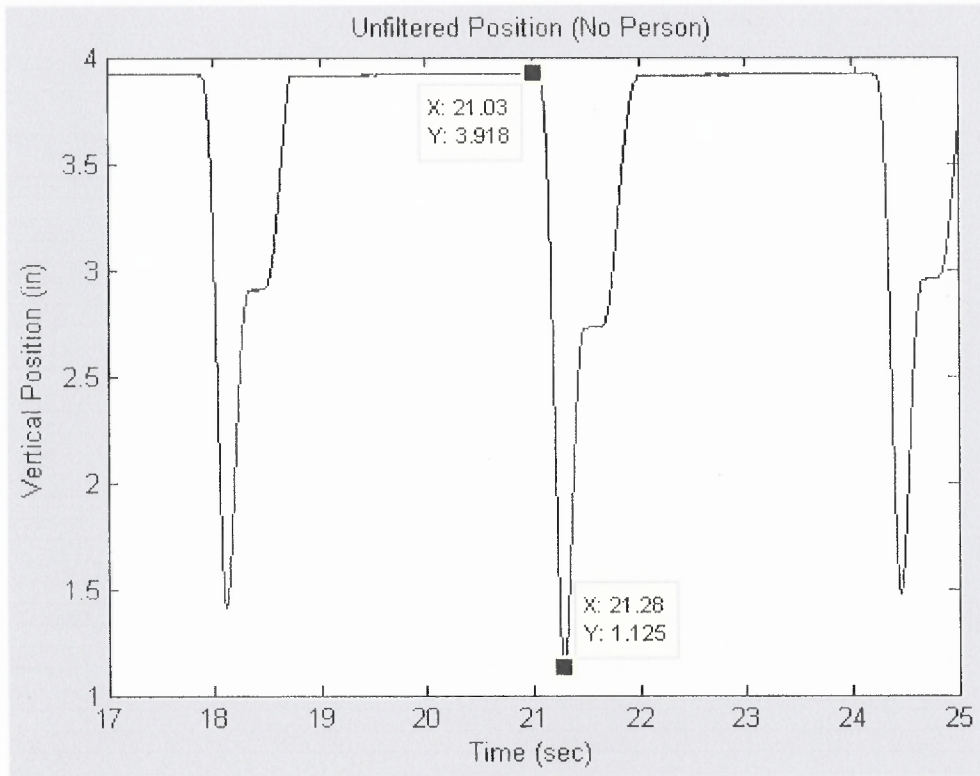


Figure 4.8 Portion of position data collected for zero load.

Figures 4.9 and 4.10 show 15 seconds of data collected without loading and while allowing the device to fall for the entire four inch descent without attempting to cushion the impact. As during the zero loading case with applying air for cushioning the free-fall, the device achieves its maximum downward acceleration approximately 100 milliseconds after it began its initial descent. Likewise the maximum downward velocity occurs at nearly 150 milliseconds following the beginning of the downward motion. However, the difference between the no cushioning and cushioning scenarios lies in the position at which each of these extremes occur. Compared to when air is applied, when no cushioning is administered the device falls an extra quarter of an inch before reaching its maximum downward acceleration. It achieves a downward acceleration of approximately 20 ft/s^2 . Likewise, its maximum downward velocity occurs at a half inch

lower than when air is applied to raise the actuator. Its maximum downward velocity is approximately 7 in/s greater than the air cushioning case. Also of importance is the lack of a rebound as seen when air is applied. Even though the air still compresses due to the area of the exhaust port being smaller than the area of the cylinder bore, the system is always open to the air, which in turn prevents any rebound from the compressed air.

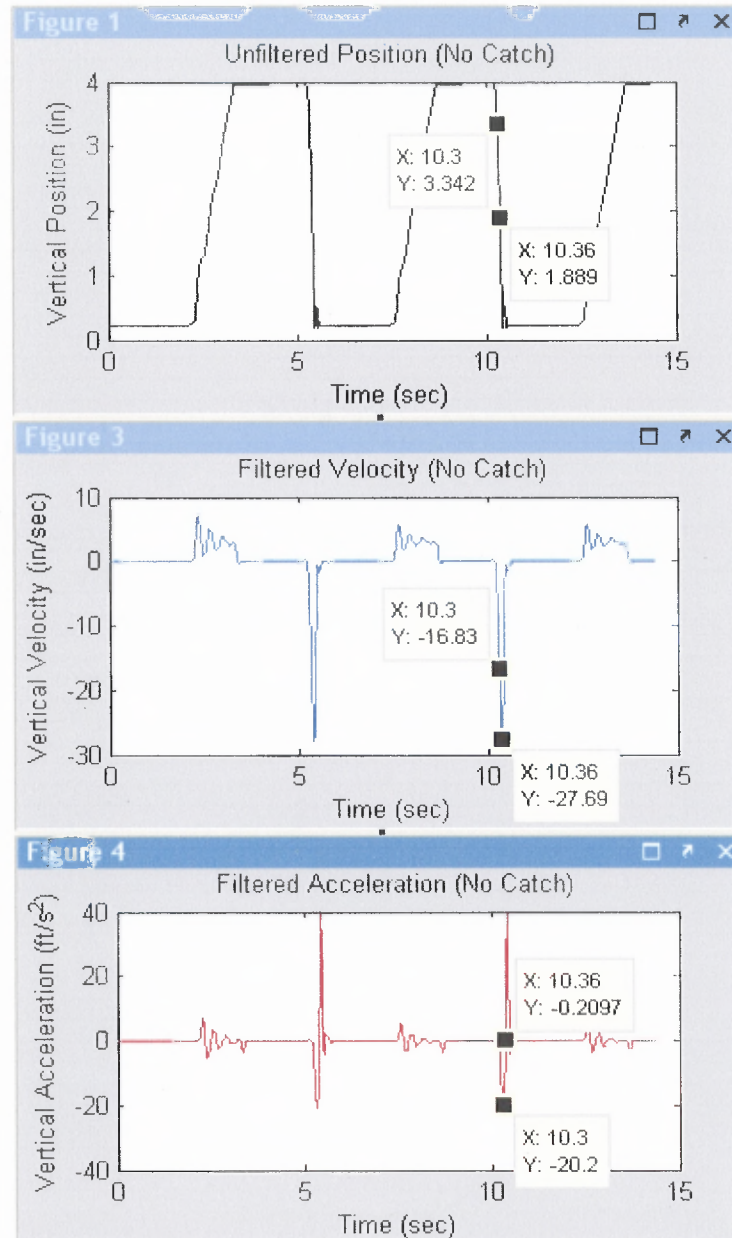


Figure 4.9 Position, velocity, and acceleration data collected for zero load without applying an upward air pressure to catch the free-fall.

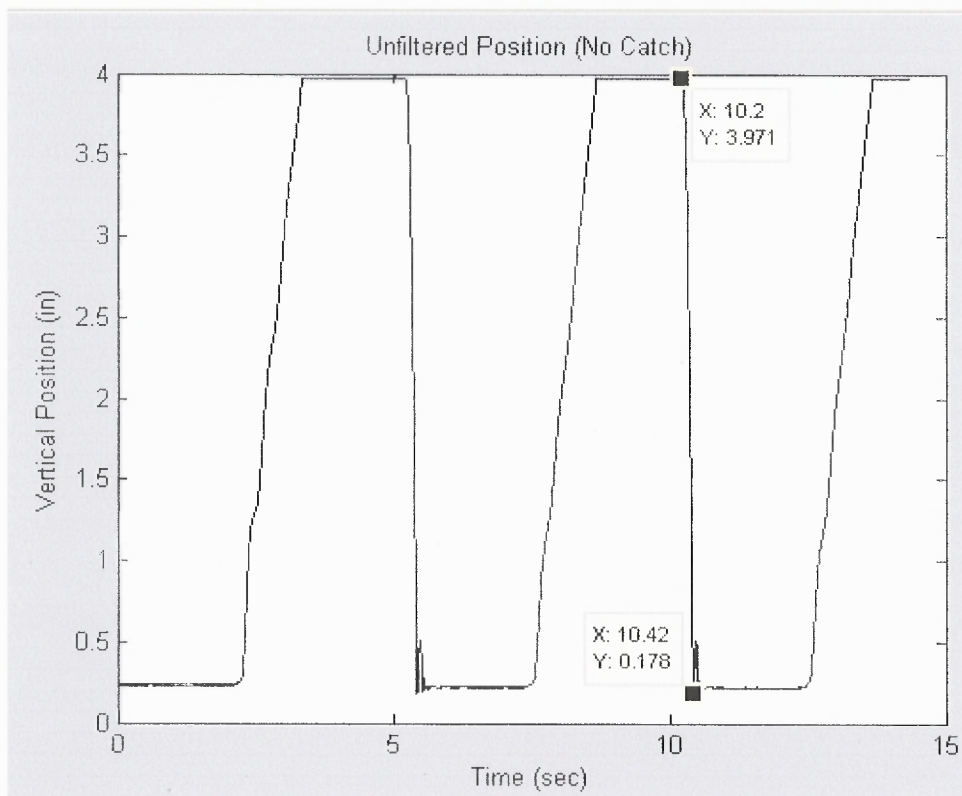


Figure 4.10 Position data collected for zero load without applying an upward air pressure to catch the free-fall.

CHAPTER 5

CONCLUSIONS AND FURTHER IMPROVEMENTS

In its current state, the otolith stimulation platform makes it possible for otolith stimulation experiments to be safely conducted on subjects weighing up to 180 pounds. Considering the direct acting control valves are rated for pressures up to 90 psi and the pressure applied to raise the 180 pound person was 75 psi, the device can theoretically operate correctly with even larger loads applied. This provides a large range of subjects on which this device could be used to conduct research. An improvement to the design that would make it possible to subject even heavier subjects to stimulation with this device would be to replace the direct acting control valves that are rated for up to 90 psi with control valves with a higher pressure rating. For the research that this device was designed for, this is an unnecessary alteration.

As stated earlier, the device achieves approximately half of Earth's gravitational acceleration. This meets the design goal of achieving at least half of the acceleration due to gravity. An acceleration closer to full gravitational acceleration would be optimal; however, the reason for this decreased acceleration is largely due to the system being comprised of pneumatics and so the device has been optimized to perform at its peak capabilities. In addition to air resistance, friction from the actuator piston may also factor into the decreased performance. Increasing the rigidity of the device may reduce any friction forces from the piston rod; however, since the acceleration of the system was approximately half of Earth's gravitational acceleration for all three loading cases and the maximum downward velocity of the device remained approximately constant regardless

of loading, it can be concluded that friction has a minimal effect on the overall performance of the device. As discussed earlier, friction from the guide block and rail system is negligible. An improvement to the design for achieving acceleration values closer to that of Earth's acceleration would be to increase the stroke length of the pneumatic air cylinders. By increasing the stroke length, the device would be capable of free-falling for a greater length of time before turning the air on to stop the free-fall and raise the device. This was confirmed by comparing the two cases when air was and was not applied to stop the free-fall. The acceleration reached a value considerably closer to the acceleration due to gravity. On the other hand, by increasing the stroke length, the piston would be more likely to deflect and bind, although the rigidity of the device will most likely prevent this deflection.

Overall, the device in its present state is ready to be used to conduct research that requires stimulation of the otolith organs.

APPENDIX A

CONTROL VALVE SPECIFICATIONS

Figures A.1 and A.2 provide general specifications for the Isonic MOD3 control valves.

Control Valves

Isonic™ MOD 3+

Valve Data

Product / Function	Flow (L/min)	Pressure Range	Vacuum	Orifice Size	Tubing
2/2 Direct Acting or 3/2 Direct Acting	A: 0.03	0-120 PSI (0-8.3 Bar)	Full	A: 0.04 (1.0 mm)	ALL MODELS 1/4" (6mm) O.D. Ports 1, 2, 3, 4 5/32" (4mm) Port 14 Optional
	B: 0.06	0-100 PSI (0-6.9 Bar)	Full	B: 0.06 (1.5 mm)	
	C: 0.11	0-90 PSI (0-6.2 Bar)	Full	C: 0.08 (2.0 mm)	
4/2 Single Solenoid Pilot Operated	0.80	30-100 PSI (2.0-8.3 Bar)	Full with External Pilot	0.21" (5.3 mm)	
4/2 Double Solenoid Pilot Operated	0.80	15-100 PSI (1.0-8.3 Bar)	Full with External Pilot	0.21" (5.3 mm)	

General

Temperature Range : 0°- 120° F (-18° C to + 50° C)

Media: Air or Inert Gas

Lubrication: Not Recommended

Filtration: 3 micron

Duty: 100%

Manual Override: Standard (Pilot Models)

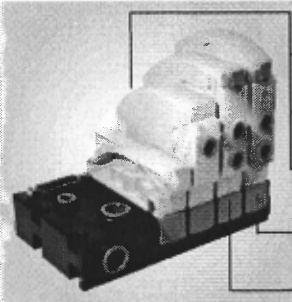
Collets: 1/4" (6 mm) and 5/32" (4mm)

Voltages: DC: 12 V and 24 V
AC: 24 V, 110 V @ 50 / 60 Hz

Seals: Viton® and Nitrile

Body: GE Thermoplastic

Response Time: 10 ms On; 35 ms Off



Valve Symbols

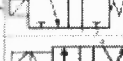
	2/2 NC
	3/2 NC
	3/2 NO
	4/2 Double Solenoid
	4/2 Single Solenoid

Figure A.1 Isonic MOD3 valve data. [19]

Control Valves

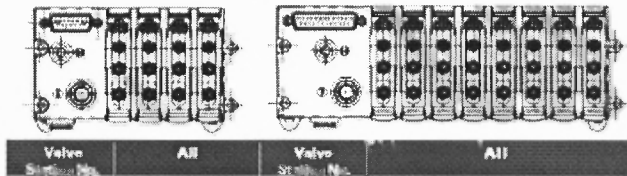
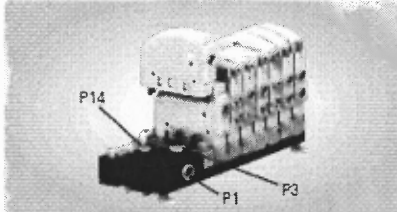
Isonic[®] MOD 3⁺

General Information

Flow Connections 120 PSI (8.3 Bar)			Electrical Connections	Mounting Options
Supply (Port 1)	Exhaust (Port 3)	Pilot (Port 14)	Sub-D Type	Panel Front Mounting
A=3/8"	A=3/8"	A=1/4"	15 Pin =	Panel Rear Mounting
B=	B=	B=	25 Pin =	35mm DIN Rail w/ Optional Kit
10mm	10mm	6mm	9 Valve Station	

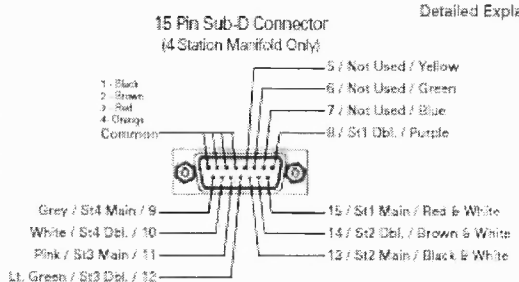
Manifold Sub-D Connections

15 Pin +VE Signal					25 Pin +VE Signal								
Valve Station No.	1	2	3	4	Valve Station No.	1	2	3	4	5	6	7	8
Valve Type	Pin Connection No.				Valve Type	Pin Connection No.							
Direct Acting Sol.	15	12	11	9	Direct Acting Sol.	11	13	24	22	20	18	16	14
Single and Double Sol. Pilot 1 > 4	15	12	11	9	Single and Double Sol. Pilot 1 > 4	11	13	24	22	20	18	16	14
Double Sol. Pilot Port 1 > 2	8	14	12	10	Double Sol. Pilot Port 1 > 2	10	12	25	23	21	19	17	15

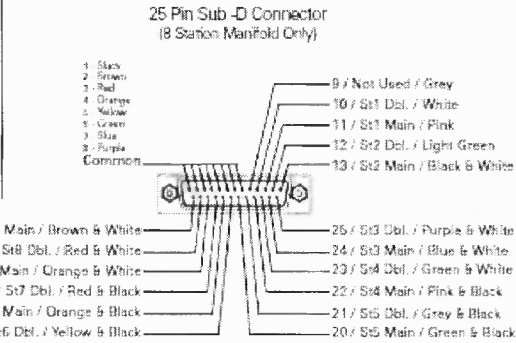


NOTE: Valve 1 is located nearest to Serial Connector, Common Pins are connected internally

Wiring / 15 & 25 PIN Detail - Cable End (Colors indicated apply to Mead accessories P1*-15SDC and P1*-25SDC)
 Numbers near pin lines are the pin numbers. Center information refers to usage (see detailed explanation). Colors indicated on the outside are the wire color of the Mead accessories.



Detailed Explanation: St1 Main = Station 1, Main connection (Used for all valves installed here).
 St1 Dbl. = Station 1, Double Solenoid Connection (The second connection for a double solenoid type valve - This is only used for the double solenoid type. Remember double solenoids have two connections.)



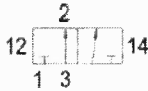
NOTE: All Commons are connected internally on both the 4 and 8 Station Manifolds. 28 AWG wire.

Figure A.2 Isonic MOD3 manifold and wiring information. [19]

Figure A.3 provides general specifications for the Alkon Corporation series P 3-way control valves.

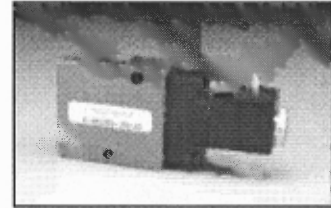


SERIES P-MC 3-WAY VALVES



GENERAL INFORMATION

- Compact size
- Variety of combinations
- In line design - or mount on manifold
- Normally open or normally closed models
- 1/8 NPT or 1/4 NPT ports
- Cv - .5 (1/8") or .85 (1/4")
- Cycle Rate - Up to 2,500 per minute
- Standard locking manual override



SIMPLE HOW-TO-ORDER INSTRUCTIONS

P-M	C	1	SS	115/60	HW
SERIES	TYPE	SIZE	FUNCTION	VOLTAGE	OPTIONS
P	MC (NC) MO (NO)	1 (1/8 NPT) 2 (1/4 NPT)	SS-Single Solenoid SP-Single Pilot	6 VDC 24/60 12 VDC 115/60 24 VDC 230/60	HW - Hard Wire Coil Leads FA - Factory Assembly of Manifolds XP - External Pilot Supply Port

Figure A.3 Alkon Corporation series P 3-way control valve specifications. [20]

APPENDIX B

NI DAQCARD-6024E SPECIFICATIONS

This Appendix lists the specifications of the NI DAQCard-6024E (for PCMCIA)

Table B.1 National Instruments DAQCard-6024E Analog I/O Specifications [21]

Analog Input	
Number of Channels	16 SE/8 DI
Sample Rate	200 kS/s
Resolution	12 bits
Simultaneous Sampling	No
Maximum Voltage Range	-10..10 V
Range Accuracy	19.112 mV
Minimum Voltage Range	-50..50 mV
Range Accuracy	0.119 mV
Number of Ranges	4
On-Board Memory	2048 samples
Analog Output	
Number of Channels	2
Update Rate	1 kS/s
Resolution	12 bits
Maximum Voltage Range	-10..10 V
Range Accuracy	10.568 mV
Minimum Voltage Range	-10..10 V
Range Accuracy	10.568 mV
Current Drive (Channel/Total)	5 mA/10 mA

Table B.2 National Instruments DAQCard-6024E Digital I/O Specifications [21]**Digital I/O**

Number of Channels	8 DIO
Timing	Software
Logic Levels	TTL
Maximum Input Range	0..5 V
Maximum Output Range	0..5 V
Input Current Flow	Sinking, Sourcing
Programmable Input Filters	No
Output Current Flow	Sinking, Sourcing
Current Drive (Channel/Total)	24 mA/192 mA
Watchdog Timer	No
Supports Programmable Power-Up States?	No
Supports Handshaking I/O?	No
Supports Pattern I/O?	No

Table B.3 National Instruments DAQCard-6024E Counter/Timers Specifications [21]

Counter/Timers	
Number of Counter/Timers	2
Resolution	24 bits
Maximum Source Frequency	20 MHz
Minimum Input Pulse Width	10 ns
Logic Levels	TTL
Maximum Range	0..5 V
Timebase Stability	100 ppm
GPS Synchronization	No
Pulse Generation	Yes
Buffered Operations	Yes
Debouncing/Glitch Removal	No
Timing/Triggering/Synchronization	
Synchronization Bus (RTSI)	No
Triggering	Digital

APPENDIX C

NI DAQCARD-6024E ACCESSORIES SPECIFICATIONS

This Appendix lists the specifications of the accessories to the NI DAQCard-6024E (for PCMCIA) that were used during operation of the device.

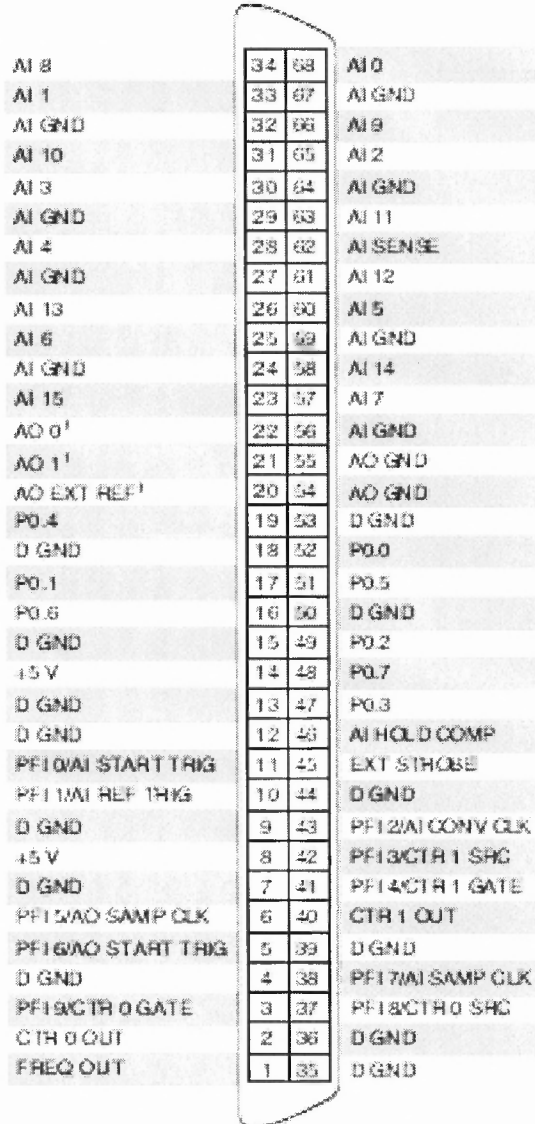


Figure C.1 National Instruments SH68-68-EP cable I/O connector diagram. [22]

68 ACH0	61 ACH12	15 DGND	08 +5V	01 FREQ_OUT
34 ACH8	27 AIGND	49 DIO2	42 GPCTR1_SRC	35 DGND
67 AIGND	60 ACH5	16 DIO6	9 DGND	2 GPCTR0_OUT
33 ACH1	26 ACH13	50 DGND	43 CONVERT	36 DGND
66 ACH 9	59 AIGND	17 DIO1	10 TRIG2	3 GPCTR0_GATE
32 AIGND	25 ACH6	51 DIO5	44 DGND	37 GPCTR0_SRC
65 ACH2	58 ACH14	18 DGND	11 TRIG1	4 DGND
31 ACH10	24 AIGND	52 DIO0	45 EXTSTROBE	38 STARTSCAN
64 AIGND	57 ACH7	19 DIO4	12 DGND	5 WFTRIG
30 ACH3	23 ACH15	53 DGND	46 SCANCLK	39 DGND
63 ACH11	56 AIGND	20 RESERVED	13 DGND	6 UPDATE
29 AIGND	22 DACDOUT	54 AOGND	47 DIO3	40 GPCTR1_OUT
62 AISENSE	55 AOGND	NA NA	14 +5V	7 DGND
28 ACH4	21 DAC1OUT	NA NA	48 DIO7	41 GPCTR1_GATE

Figure C.2 National Instruments CB-68LP connection block layout. [23]

APPENDIX D

REED RELAY SPECIFICATIONS

This Appendix describes the specifications of the compact 5VDC/1A SPST reed relay purchased from RadioShack Corporation for operation of this device.

Table D.1 Compact 5VDC/1A SPST Reed Relay General Features [24]

Type	OMR-112H
Application	UL E822922
Rated coil voltage	5 VDC (at 20°C)
Operating voltage	3.5 VDC (at 20°C)
Release voltage	0.5 VDC (at 20°C)
Maximum applicable voltage	8 VDC (at 20°C)
Maximum switching power	10 (watt/VA)
Maximum switching voltage	60 VDC, 120VAC
Maximum switching current	0.5 A
Maximum initial contact resistance	150m ohms

Table D.2 Compact 5VDC/1A SPST Reed Relay Technical Specifications [24]

Model	275-232
Product Type	SPST
Enclosure Color	BLUE
Body Material	Multi
Fits What	
Model	275-232
Miscellaneous Features	
Min Operating Temperature	-30 Fahrenheit
Max Operating Temperature	70 Fahrenheit
Shock Tolerance	20G(11ms)
Vibration Tolerance	20G
Supported Languages	English

APPENDIX E

PNEUMATIC AIR CYLINDER SPECIFICATIONS

This Appendix contains the specifications of the Bimba position feedback cylinders incorporated into this design.

Nose Mount

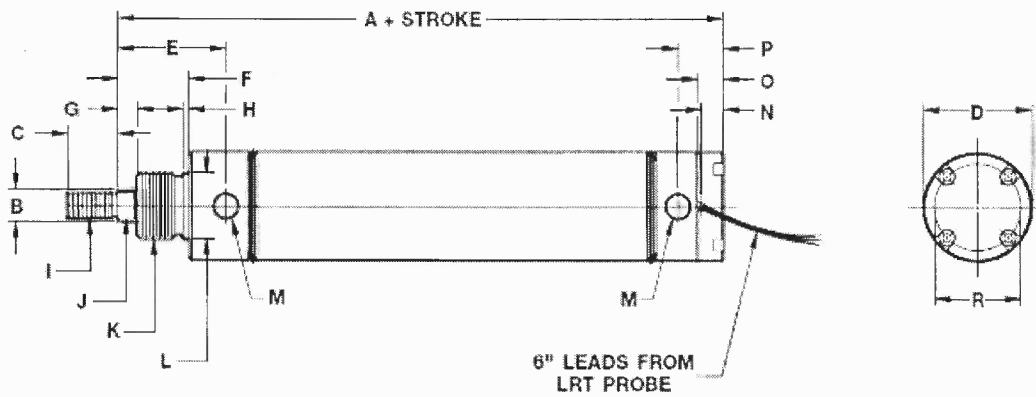


Figure E.1 Pneumatic actuator with assigned dimension variables. [25]

Table E.1 Dimension Values for Bimba Position Feedback Cylinder [25]

Dimensions (in.)

	1-1/16" Bore (09)		1-1/2" Bore (17)	2" Bore (31)	2-1/2" Bore (50)	3" Bore (70)
A	4.59		4.88	5.72	6.41	6.78
B	Ø 0.38		Ø 0.50	Ø 0.63	Ø 0.75	Ø 0.75
C	0.63		0.88	1.00	1.25	1.25
D	Ø 1.31		Ø 1.58	Ø 2.09	Ø 2.58	Ø 3.13
E	1.75	Option L 1.52	1.72	2.10	2.28	2.53
F	1.06		1.13	1.38	1.50	1.69
G	0.31		0.31	0.38	0.44	0.44
H	0.08		0.09	0.11	0.13	0.13
I	3/8-24 UNF		7/16-20 UNF	1/2-20 UNF	5/8-18 UNF	5/8-18 UNF
J	0.31		0.44	0.50	0.63	0.63
K	7/8-14 UNF		1-1/8-12 UNF	1-1/4-12 UNF	1-3/8-12 UNF	1-1/2-12 UNF
L	Ø 0.87		Ø 1.12	Ø 1.25	Ø 1.37	Ø 1.62
M	1/8 NPT		1/4 NPT	1/4 NPT	3/8 NPT	3/8 NPT
N	0.36		0.36	0.42	0.48	0.55
O	0.44		0.44	0.50	0.56	0.63
P	0.84		0.81	0.88	1.12	1.88
Q	0.62		0.74	0.86	0.99	0.99
R	Ø 1.09		Ø 1.36	Ø 1.67	Ø 2.06	Ø 2.44
S	0.47		0.56	0.66	0.75	0.81
T	5.06		5.44	6.38	7.16	7.60
U	5.44		5.91	6.88	7.78	8.22
V	Ø 0.31		Ø 0.38	Ø 0.44	Ø 0.50	Ø 0.50
W	0.88		1.25	1.44	1.88	2.25
X	1.38		1.75	2.25	2.75	3.25
Y	0.75		0.69	0.75	0.88	0.94
Z	0.88		0.75	1.00	1.25	1.38
AA	1.63	Option L 1.52	1.68	1.75	2.13	2.31
BB	2.03		2.00	2.41	2.72	2.91
CC	#10		1/4	3/8	7/16	1/2
DD	Ø 0.33		Ø 0.41	Ø 0.58	Ø 0.67	Ø 0.77
EE	0.20		0.25	0.39	0.45	0.52

Table E.2 Wiring Chart for Position Feedback Cylinders [25]

3-pin Connector

Wire Colors

WIRES	6" LEADS	PLUG
Input	Red	Blue
Ground	Black	Black
Output	White	Brown

Engineering Specifications

Repeatability:	±0.001" Cylinder Only. Refer to specifications in the following sections for positioning or measuring repeatability. Power supply ripple and A/D error may reduce repeatability when PFC is utilized with industrial control systems.
Nonlinearity:	± 1 percent of full stroke
Resolution:	Infinite
Signal Input:	10 VDC typical
Input Impedance Required:	1 MΩm
Signal Output:	> 0 to slightly less than FS signal input (The nominal electrical stroke is slightly larger than the mechanical stroke of cylinder)
Maximum speed:	25 in./sec.
Rated Life of LRT Wiper:	1,000 ¹ miles of travel
Rated Life of Probe:	10 million cycles ¹
Air Requirements:	Filtered to 5 micron with 0 degree dewpoint recommended. Moisture inside cylinder will cause output signal fluctuation.
Pressure Rating:	150 psi
Temperature Rating:	0 ¹ to 200 ¹ F ²
Interface:	6" standard leads or optional 8mm DIN connector
Cylinder Body:	304 stainless steel
Piston Rod:	Hard chrome plated carbon steel with blackened threads and wrench flats
Rod Bushing:	Sintered bronze
End Caps:	Anodized Aluminum alloy
Piston Seal:	Internally lubricated urethane (standard) Internally lubricated Buna (L option)
Rod Wiper:	Internally lubricated Buna N (omitted on L option)
Rod Seal:	Internally lubricated Buna N (N/A on standard model)

¹Higher velocities increase wear rate.

²Special low temperature lubrication is required for positioning applications using option L seals below 35°F.

ESTIMATED CYLINDER WEIGHTS (LBS)					
	1-1/16"	1-1/2"	2"	2-1/2"	3"
PFC-	0.44	0.88	2.02	2.78	3.62
PFC-X	0.40	0.86	2.14	2.96	3.85
PFC-BF	0.54	1.07	2.28	3.02	4.08
ADDER WT:IN	0.06	0.10	0.15	0.20	0.29

Repair Parts

PART	DESCRIPTION
RPFC Bare Stroke-Options*	Replacement Cylinder
RD-53129-Stroke-Options**	Replacement Probe

* Only options required are BF, B, and L as Rear Cap is not included.

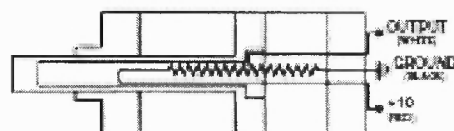
** Only option required for replacement probe is Option P.

How to Order

Add the bore size, stroke and options needed to the basic model number shown above for a replacement cylinder.

Add the stroke length to the basic model number shown above for a replacement probe. For example, a replacement probe for a 6" stroke Position Feedback Cylinder would be ordered as a RD-53129-6.

LRT CIRCUIT DIAGRAM



STROKE = 0; OUTPUT VOLTAGE = 0 VOLTS
STROKE = FULL; OUTPUT VOLTAGE = 10 VOLTS

Figure E.2 Engineering specifications for position feedback cylinders. [25]

APPENDIX F

BILL OF MATERIALS

This Appendix contains the bill of materials for this device. Descriptions and the sources of the components can be found in Tables F.1 and F.2. The quantity of each part used in the current design can be found in Tables F.3 and F.4.

Table F.1 Bill of Materials

Part Name	Part Number	Description	Supplier	Identifier
T-Slot #1	1001	Anodized T-Slotted Aluminum Extrusion	80/20 Inc.	1515-LITE
T-Slot #2	1002	Anodized T-Slotted Aluminum Extrusion	80/20 Inc.	1515-LITE
T-Slot #3	1003	Anodized T-Slotted Aluminum Extrusion	80/20 Inc.	1515-LITE
T-Slot #4	1004	Anodized T-Slotted Aluminum Extrusion	80/20 Inc.	1515-LITE
Horizontal Support Tube #1	1005	1.5" x 3" Anodized Rectangular Tube	80/20 Inc.	8120
Horizontal Support Tube #2	1006	1.5" x 3" Anodized Rectangular Tube	80/20 Inc.	8120
Horizontal Support Tube #3	1007	1.5" x 3" Anodized Rectangular Tube	80/20 Inc.	8120
Horizontal Mounting Tube	1008	1.5" x 3" Anodized Rectangular Tube	80/20 Inc.	8120
Vertical Support Tube #1	1009	1.5" x 3" Anodized Rectangular Tube	80/20 Inc.	8120
Vertical Support Tube #2	1010	1.5" x 3" Anodized Rectangular Tube	80/20 Inc.	8120
Vertical Mounting Tube	1011	1.5" x 3" Anodized Rectangular Tube	80/20 Inc.	8120
Connecting Tube	1012	1.5" x 3" Anodized Rectangular Tube	80/20 Inc.	8120
L Joining Plate	1013	5 Hole "L" Joining Plate	80/20 Inc.	4481
T Joining Plate	1014	5 Hole "T" Joining Plate	80/20 Inc.	4480
Economy T-Nut Assembly	1015	5/16"-18 Economy T-Nut Assembly	80/20 Inc.	3320
Double T-Nut Assembly	1016	5/16"-18 Double T-Nut Assembly	80/20 Inc.	3355
Triple T-Nut Assembly	1017	5/16"-18 Triple T-Nut Assembly	80/20 Inc.	3357
Economy T-Nut	1018	5/16"-18 Economy T-Nut (Stainless Steel)	80/20 Inc.	3678
Standard T-Nut	1019	1/4"-20 Standard T-Nut	80/20 Inc.	3202
Leveling Foot	1020	5/16"-18 Economy Leveling Foot	80/20 Inc.	2195
Actuator	1021	Position Feedback Cylinder, 4" Stroke, 1.5" Bore, Low Friction	Bimba	PFC-174-BL
Actuator Mounting Bracket	1022	1-3/4" Bore Mounting Bracket	Bimba	D-8318
Actuator Mounting Nut	1023	1-3/4" Bore Mounting Nut	Bimba	D-8484
Actuator Mounting Bolt	1024	18-8 SS 5/16"-18 FBHSCS, 5/8" L	McMaster-Carr	97654A304
Rail Mounting Bolt	1025	18-8 SS 1/4"-20 SHCS w/ Lock Washer, 1" L	McMaster-Carr	94912A465
Guide Block Lock Washer	1026	Zinc-Plated Steel M6 Spring Lock Washer, 11.8mm OD	McMaster-Carr	91202A234
Guide Block Flat Washer	1027	Zinc-Plated Steel Large-Dia M6 Flat Washer, 18mm OD	McMaster-Carr	91100A150
Guide Block Bolt	1028	Metric Class 12.9 M6X14 SHCS Alloy Steel, 1mm Pitch	McMaster-Carr	91290A319
Frame Mount Locknut	1029	Nylon-Insert 1/4"-20 Hex Flange Locknut Zinc-Plated Steel	McMaster-Carr	93298A110
Frame Mount Bolt	1030	Black-Oxide Alloy Steel 1/4"-20 SHCS, 7/8" L	McMaster-Carr	91251A541
Frame Mount Lock Washer	1031	Zinc-Plated Steel Spring 1/4" Lock Washer, .49" OD	McMaster-Carr	91102A750
Frame Mount Flat Washer	1032	Extra-Thick High-Strength Steel 1/4" Flat Washer, 5/8" OD	McMaster-Carr	98025A029
Guide Block	1033	83.1 mm Versa-Mount Guide Block Threaded-Hole	McMaster-Carr	6709K16
Rail	1034	220 mm Rail for 83.1 mm Versa-Mount Guide Block	McMaster-Carr	6709K501
Piston Mounting Bracket	1035	6061-T6 Aluminum Flat Stock, 2.5" x 0.5", Anodized	80/20 Inc.	8337
Piston Mounting Nut	1036	7/16"-20 Hex Nut, 11/16" W, 3/8" H	McMaster-Carr	90473A220
Piston Mounting Lock Washer	1037	Zinc-Plated Steel 7/16" Spring Lock Washer	McMaster-Carr	91102A765

Table F.2 Bill of Materials (Continued)

Part Name	Part Number	Description	Supplier	Identifier
Control Valve #1	1038	Isonic MOD3 Direct Acting 3/2 Control Valve	Mead Fluid Dynamics	V3A-C131AE1
Control Valve Station	1039	Isonic MOD3 4 Station Manifold	Mead Fluid Dynamics	M5A-040411
Control Valve #2	1040	Alkon Series P 3-Way Normally Open Control Valve	Alkon Corp.	P-MO2SS-115/60
Manifold #1	1041	Aluminum Manifold w/ 4 Outlets, 1/4" NPT Inlet X 1/8" NPT Outlet	McMaster-Carr	5469K121
Manifold #2	1042	Aluminum Manifold w/ 4 Outlets, 3/8" NPT Inlet X 1/4" NPT Outlet	McMaster-Carr	5469K123
Tube Fitting #1	1043	3/8" Tube OD X 1/8" NPT Male Pipe Push-to-Connect Tube Adapter	McMaster-Carr	5779K115
Tube Fitting #2	1044	1/4" Tube OD X 1/4" NPT Male Pipe Push-to-Connect Tube Adapter	McMaster-Carr	5779K109
Tube Fitting #3	1045	1/4" Tube OD X 3/8" NPT Male Pipe Push-to-Connect Tube Adapter	McMaster-Carr	5779K111
Tube Fitting #4	1046	3/8" Tube OD X 1/4" NPT Male Pipe Push-to-Connect Tube Adapter	McMaster-Carr	5779K116
Tube Fitting #5	1047	1/4" Tube OD X 10-32 UNF Male Thread Push-to-Connect Tube Adapter	McMaster-Carr	5779K246
Tube Fitting #6	1048	3/8" Tube OD X 1/4" NPT Male Pipe Push-to-Connect Tube Swivel Wye	McMaster-Carr	5779K628
Plug #1	1049	1/4" Pipe Size Hollow Hex-Head Brass Plug	McMaster-Carr	50785K22
Plug #2	1050	3/8" Pipe Size Hollow Hex-Head Brass Plug	McMaster-Carr	50785K23
1/4" Tubing	1051	Extra-Flex Nylon 11 Tubing, .275" ID, 3/8" OD, Semi-Clear White	McMaster-Carr	5112K65
3/8" Tubing	1052	Extra-Flex Nylon 11 Tubing, .180" ID, 1/4" OD, Semi-Clear White	McMaster-Carr	5112K63
Relay	1053	Compact 5VDC/1A SPST Reed Relay, 250 Ohm	Radio Shack	275-232
DAQCard	1054	NI 6024E.PCMCIA Data Acquisition Card	National Instruments	DAQCard-6024E
Cable	1055	SHC68-68-EP Shielded Cable, 68 D-Type to 68 VHDCI Offset, 2 m	National Instruments	SHC68-68-EP
Connection Block	1056	NI CB68-LP Data Acquisition Connection Block	National Instruments	CB68-LP
Power Supply	1057	EMCO DC Power Supply Model PSV-5	EMCO	PSV-5
Breadboard	1058	Jameco Breadboard Model JE27	Jameco	JE27
Air Compressor	1059	Porter Cable 135 PSI, 6HP/25 Gal Compressor, 6.8 SCFM @90 psi	Porter Cable	CPL6025
Machining Services				
Cut To Length #1	2001	1.5" X 1.5" T-Slot Cut To Length	80/20 Inc.	7010
Cut To Length #2	2002	1.5" X 3" Tube Cut To Length	80/20 Inc.	7020
Cut To Length #3	2003	Cut To Length for 6061-T6 Aluminum Flat Stock, 2.5" x 0.5", Anodized	80/20 Inc.	7212
Tap Profile End	2004	5/16"-18 Tap Service for 24" and 12.5" Length 1515-LITE T-Slot	80/20 Inc.	7060
Tap Profile End	2005	5/16"-18 Tap Service for 6061-T6 Aluminum Flat Stock	80/20 Inc.	7253
Tap Profile End	2006	7/16"-20 Tap Service for 6061-T6 Aluminum Flat Stock	80/20 Inc.	7000 Series
Drill Hole #1	2007	.257" Diameter Drill Through	80/20 Inc.	7244
Drill Hole #2	2008	.328" Diameter Drill Through	80/20 Inc.	7246
Drill Hole #3	2009	.390" Diameter Drill Through	80/20 Inc.	7248
Drill Hole #4	2010	1" Diameter Drill Through	80/20 Inc.	7000 Series
Counterbore	2011	1" Counterbore for 6061-T6 Aluminum Flat Stock, 2.5" x 0.5", Anodized	80/20 Inc.	7040

Table F.3 Bill of Materials (Continued)

Part Name	Part Number	Quantity	Length	Units
T-Slot #1	1001	2.0000	24.0000	in
T-Slot #2	1002	8.0000	21.0000	in
T-Slot #3	1003	4.0000	12.5000	in
T-Slot #4	1004	4.0000	10.0000	in
Horizontal Support Tube #1	1005	2.0000	20.0000	in
Horizontal Support Tube #2	1006	2.0000	20.0000	in
Horizontal Support Tube #3	1007	1.0000	20.0000	in
Horizontal Mounting Tube	1008	2.0000	14.0000	in
Vertical Support Tube #1	1009	2.0000	13.0000	in
Vertical Support Tube #2	1010	2.0000	13.0000	in
Vertical Mounting Tube	1011	2.0000	11.5000	in
Connecting Tube	1012	2.0000	3.0000	in
L Joining Plate	1013	20.0000	N/A	each
T Joining Plate	1014	12.0000	N/A	each
Economy T-Nut Assembly	1015	4.0000	N/A	each
Double T-Nut Assembly	1016	36.0000	N/A	each
Triple T-Nut Assembly	1017	28.0000	N/A	each
Economy T-Nut	1018	8.0000	N/A	each
Standard T-Nut	1019	16.0000	N/A	each
Leveling Foot	1020	4.0000	N/A	each
Actuator	1021	4.0000	N/A	each
Actuator Mounting Bracket	1022	4.0000	N/A	each
Actuator Mounting Nut	1023	4.0000	N/A	each
Actuator Mounting Bolt	1024	8.0000	N/A	each
Rail Mounting Bolt	1025	16.0000	N/A	each
Guide Block Lock Washer	1026	16.0000	N/A	each
Guide Block Flat Washer	1027	16.0000	N/A	each
Guide Block Bolt	1028	16.0000	N/A	each
Frame Mount Locknut	1029	68.0000	N/A	each
Frame Mount Bolt	1030	84.0000	N/A	each
Frame Mount Lock Washer	1031	84.0000	N/A	each
Frame Mount Flat Washer	1032	84.0000	N/A	each
Guide Block	1033	4.0000	N/A	each
Rail	1034	4.0000	220.0000	mm
Piston Mounting Bracket	1035	4.0000	3.0000	in
Piston Mounting Nut	1036	4.0000	N/A	each
Piston Mounting Lock Washer	1037	4.0000	N/A	each

Table F.4 Bill of Materials (Continued)

Part Name	Part Number	Quantity	Length	Units
Control Valve #1	1038	2.0000	N/A	each
Control Valve Station	1039	1.0000	N/A	each
Control Valve #2	1040	4.0000	N/A	each
Manifold #1	1041	1.0000	N/A	each
Manifold #2	1042	1.0000	N/A	each
Tube Fitting #1	1043	4.0000	N/A	each
Tube Fitting #2	1044	5.0000	N/A	each
Tube Fitting #3	1045	1.0000	N/A	each
Tube Fitting #4	1046	4.0000	N/A	each
Tube Fitting #5	1047	4.0000	N/A	each
Tube Fitting #6	1048	4.0000	N/A	each
Plug #1	1049	5.0000	N/A	each
Plug #2	1050	1.0000	N/A	each
1/4" Tubing	1051	1.0000	10.0000	ft
3/8" Tubing	1052	1.0000	25.0000	ft
Relay	1053	2.0000	N/A	each
DAQCard	1054	1.0000	N/A	each
Cable	1055	1.0000	N/A	each
Connection Block	1056	1.0000	N/A	each
Power Supply	1057	1.0000	N/A	each
Breadboard	1058	1.0000	N/A	each
Air Compressor	1059	1.0000	N/A	each
Machining Services				
Cut To Length #1	2001	18.0000	N/A	each
Cut To Length #2	2002	15.0000	N/A	each
Cut To Length #3	2003	4.0000	N/A	each
Tap Profile End	2004	8.0000	N/A	each
Tap Profile End	2005	16.0000	N/A	each
Tap Profile End	2006	4.0000	N/A	each
Drill Hole #1	2007	176.0000	N/A	each
Drill Hole #2	2008	128.0000	N/A	each
Drill Hole #3	2009	4.0000	N/A	each
Drill Hole #4	2010	4.0000	N/A	each
Counterbore	2011	4.0000	N/A	each

APPENDIX G

MACHINED PART DRAWINGS

This Appendix consists of drawings of all of the parts that required additional machining upon receipt and prior to being incorporated into the design. Table G.1 lists all of the parts that required additional machining.

Table G.1 Parts Requiring Additional Machining

Part Name	Part Number	Quantity	Length	Units
Horizontal Support Tube #1	1005	2.0000	20.0000	in
Horizontal Support Tube #2	1006	2.0000	20.0000	in
Horizontal Support Tube #3	1007	1.0000	20.0000	in
Horizontal Mounting Tube	1008	2.0000	14.0000	in
Vertical Support Tube #1	1009	2.0000	13.0000	in
Vertical Support Tube #2	1010	2.0000	13.0000	in
Vertical Mounting Tube	1011	2.0000	11.5000	in
Connecting Tube	1012	2.0000	3.0000	in
Piston Mounting Bracket	1035	4.0000	3.0000	in

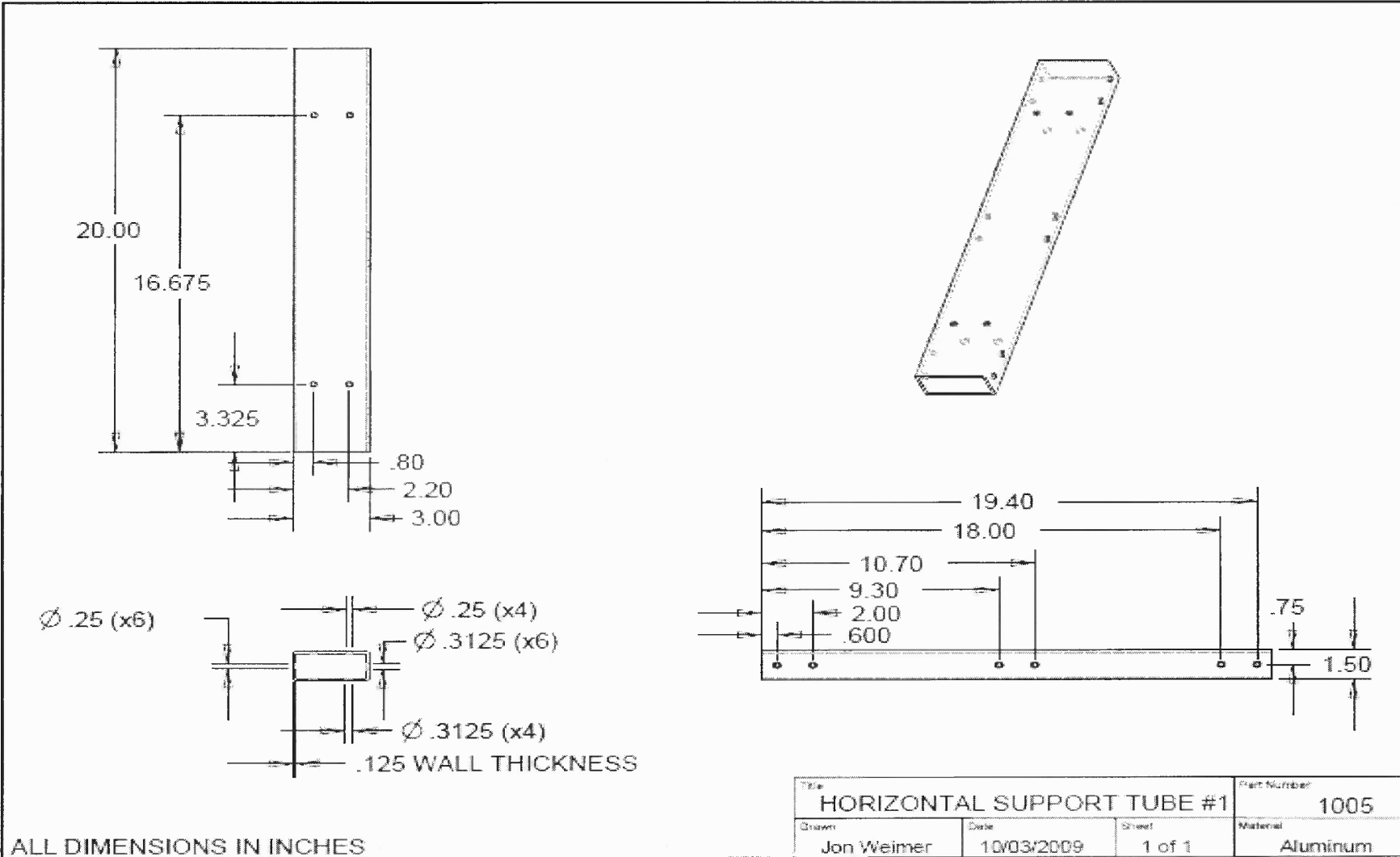


Figure G.1 Horizontal support tube #1 drawing.

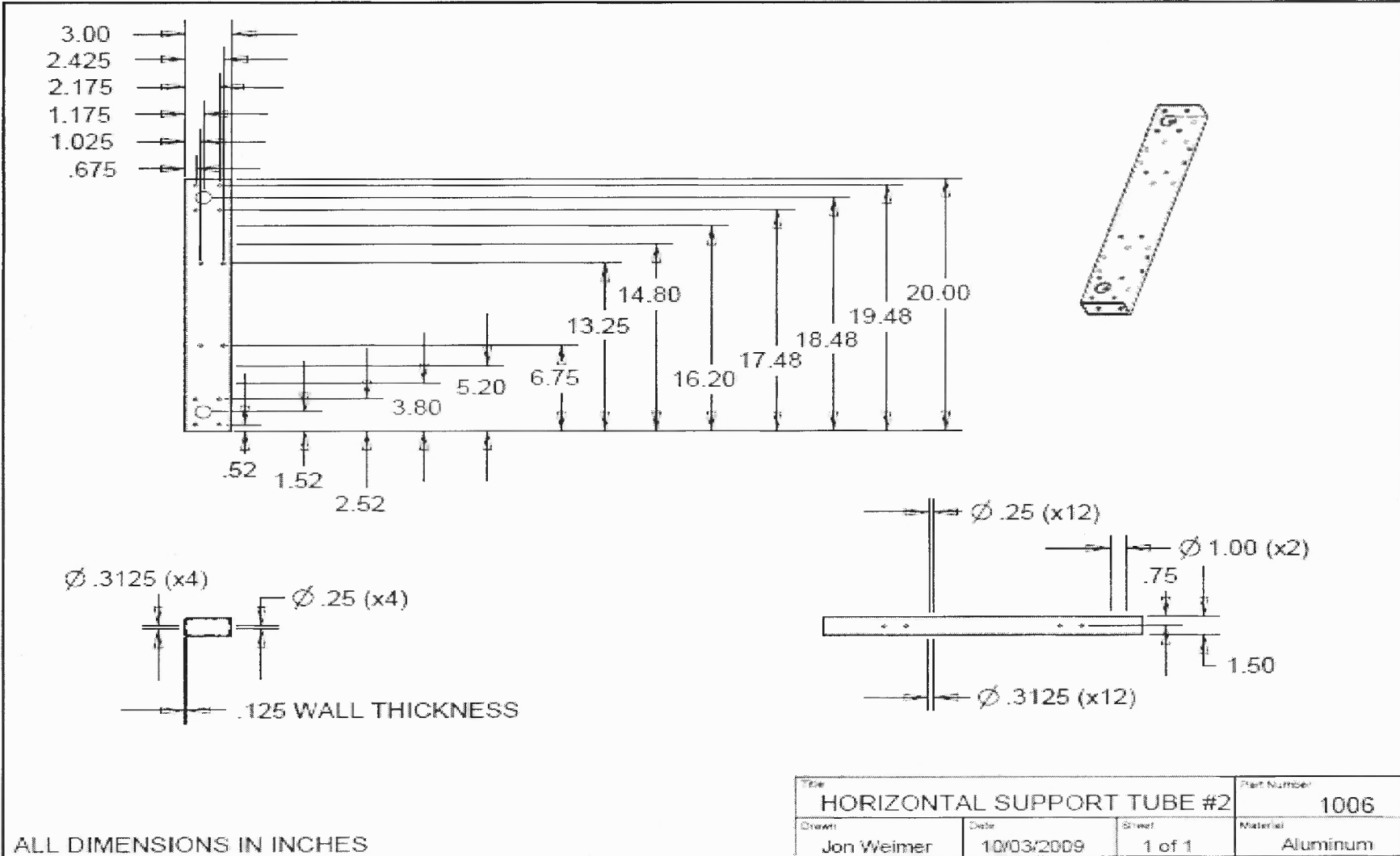


Figure G.2 Horizontal support tube #2 drawing.

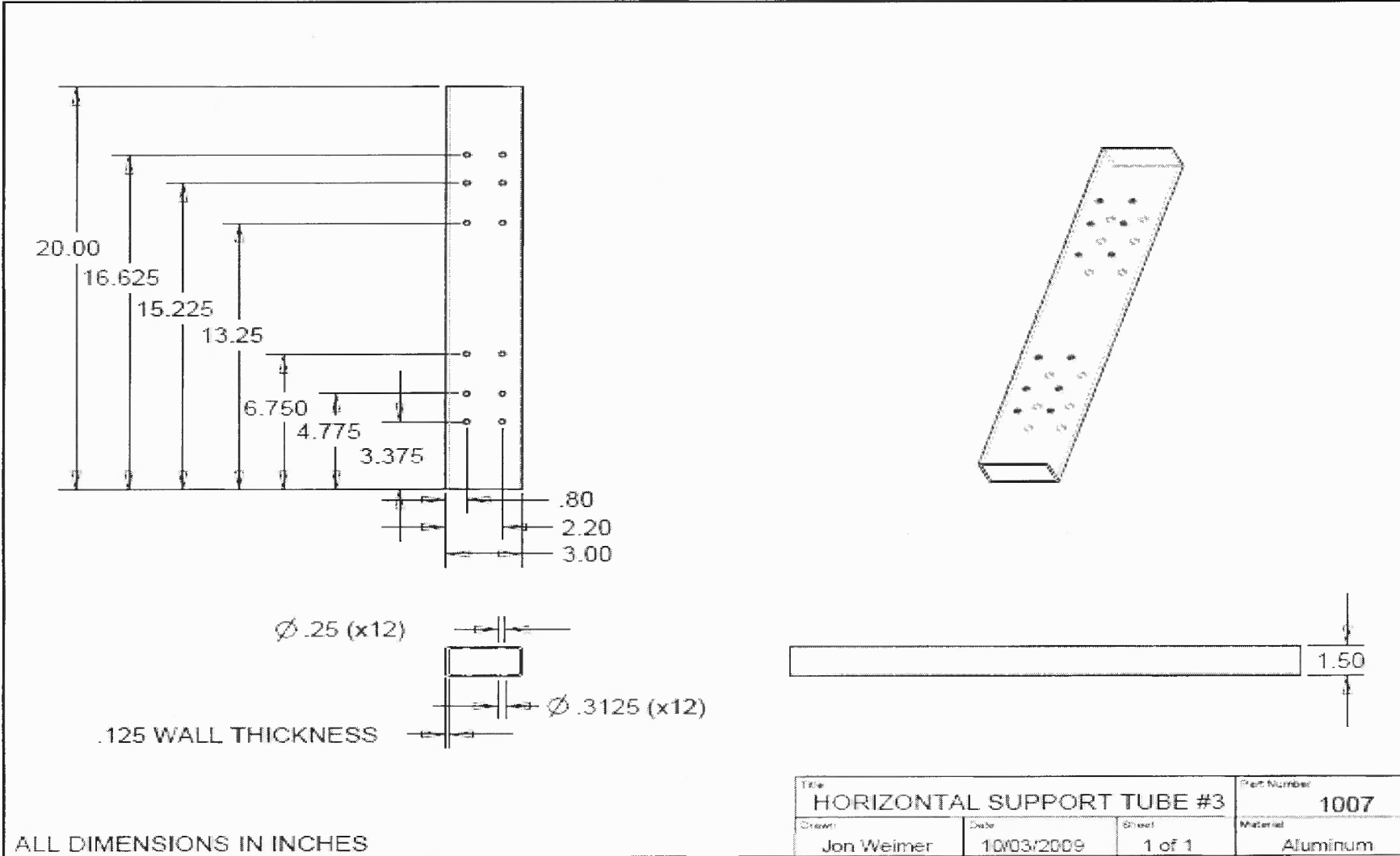


Figure G.3 Horizontal support tube #3 drawing.

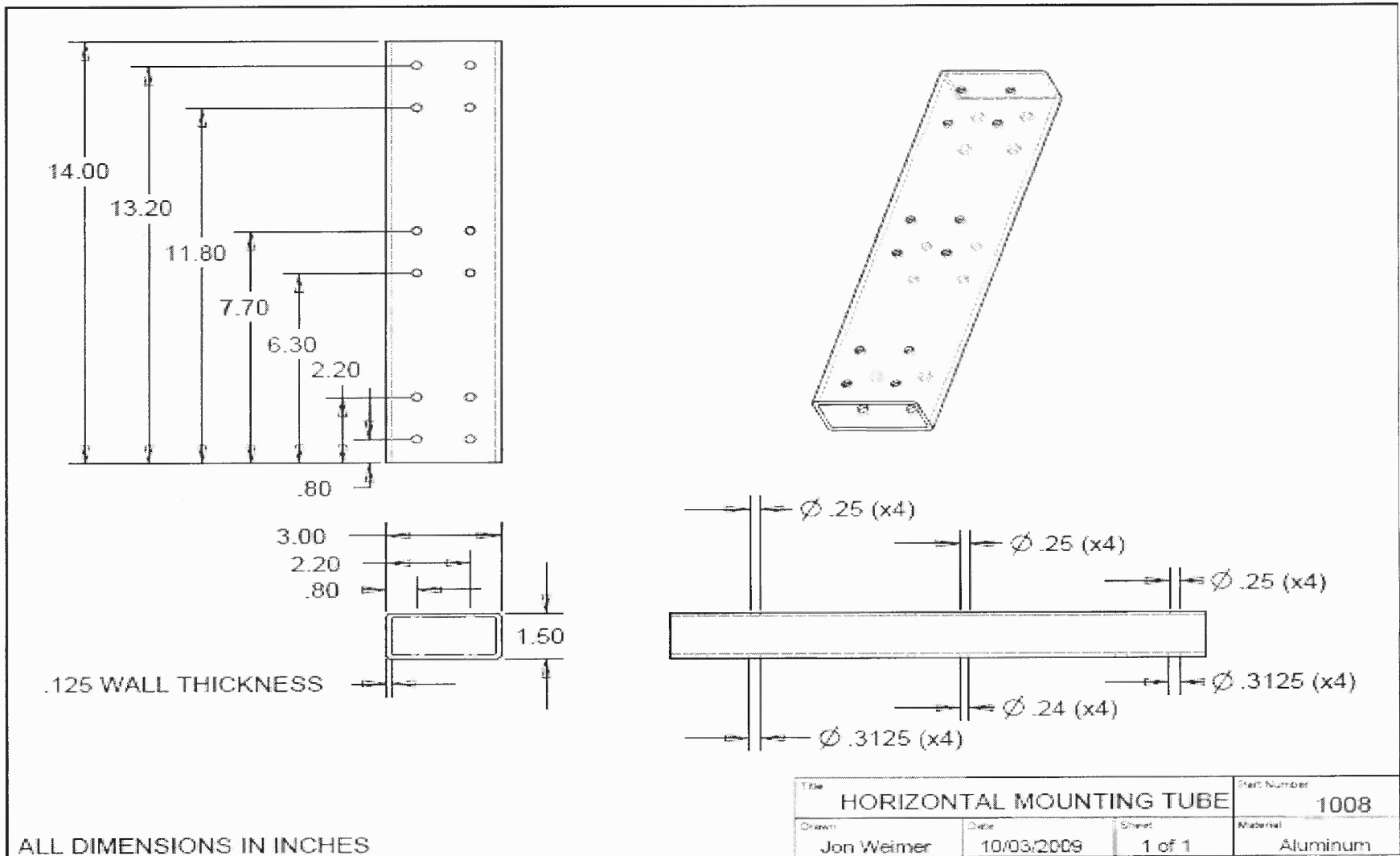


Figure G.4 Horizontal mounting tube drawing.

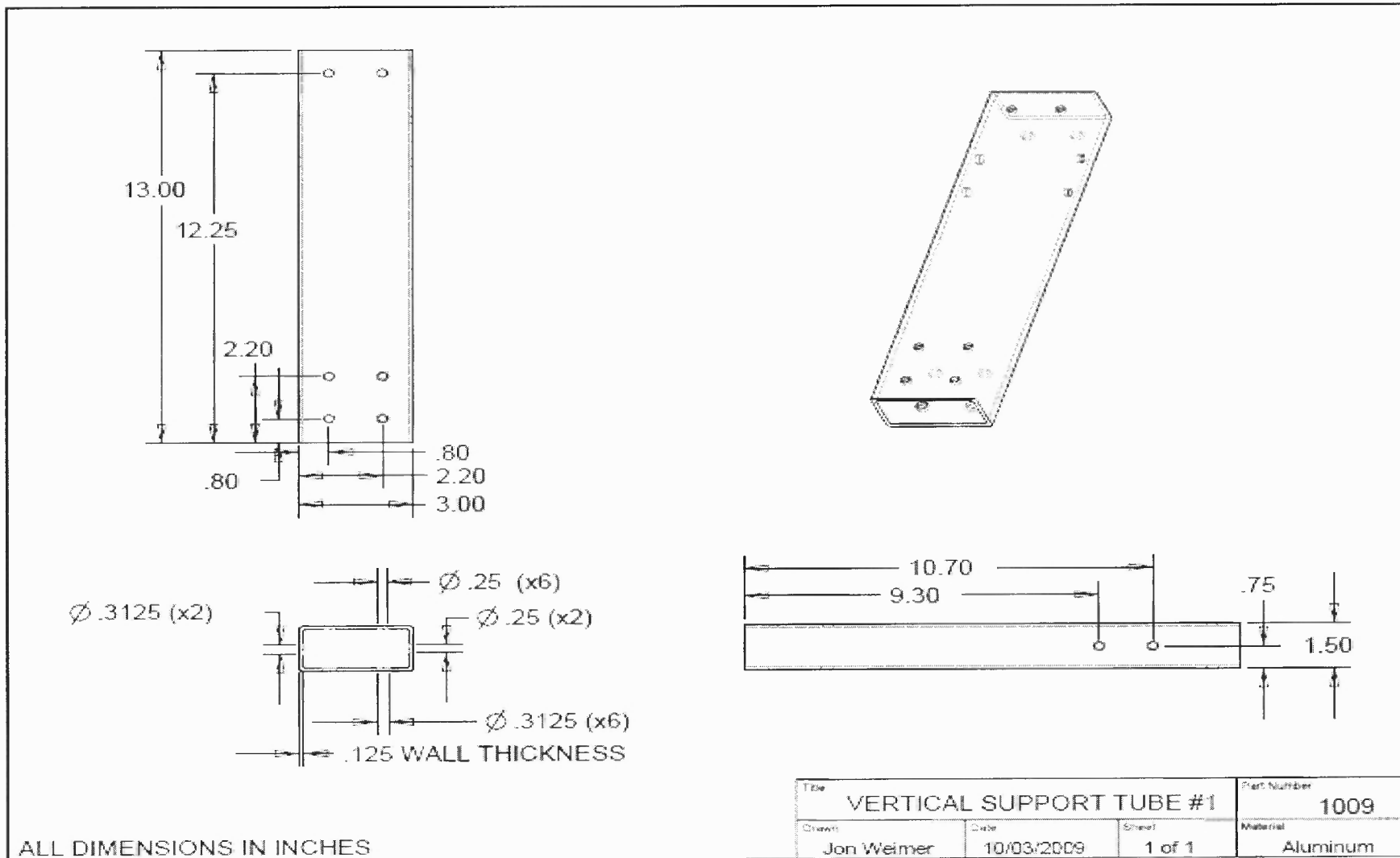


Figure G.5 Vertical support tube #1 drawing.

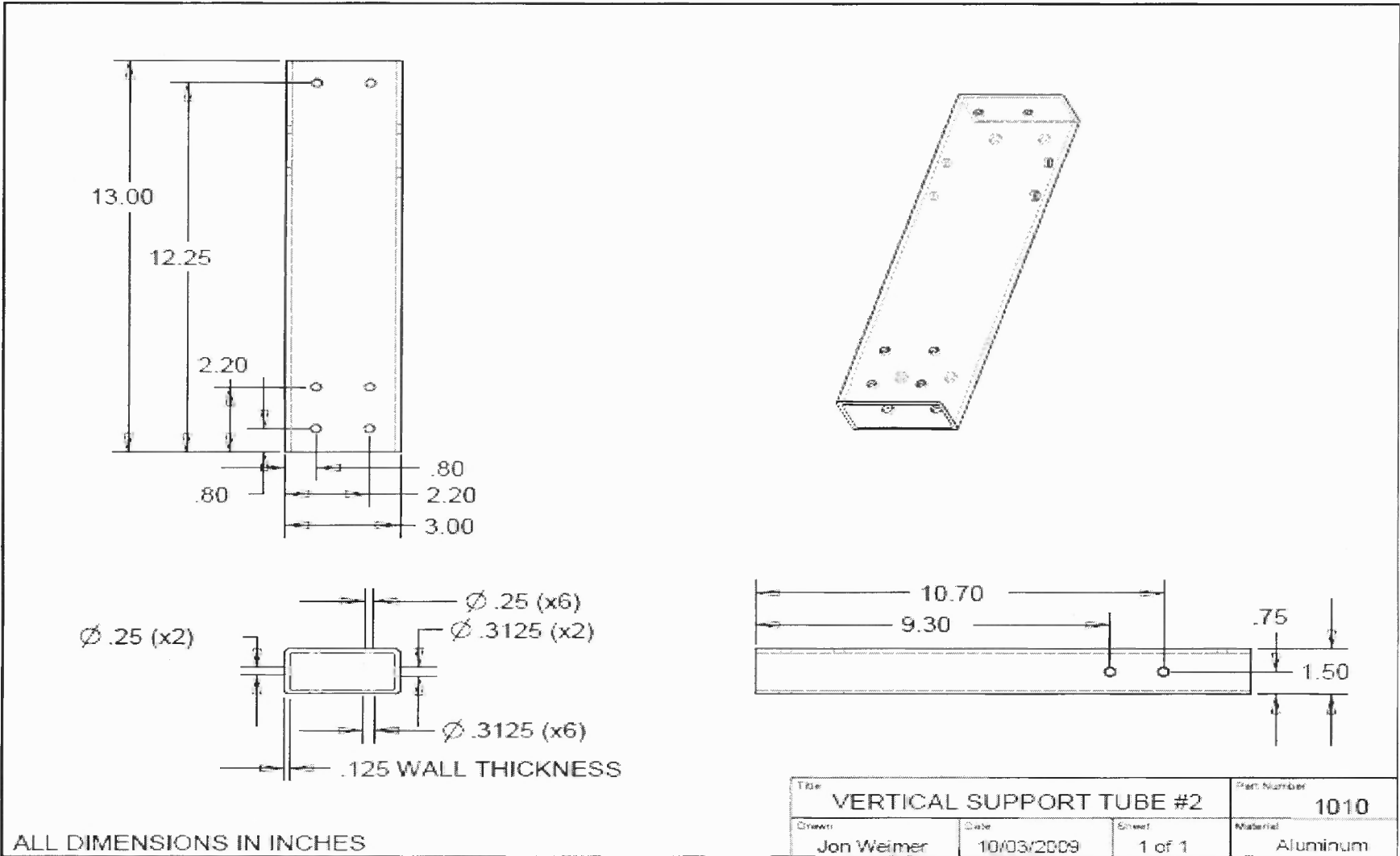
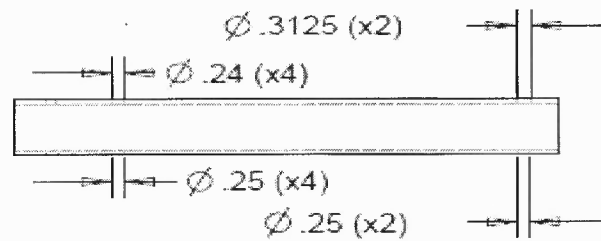
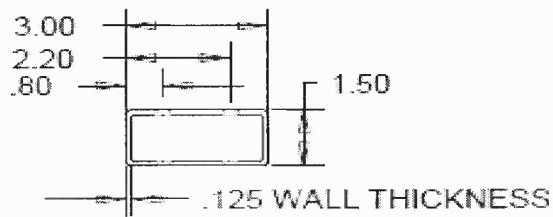
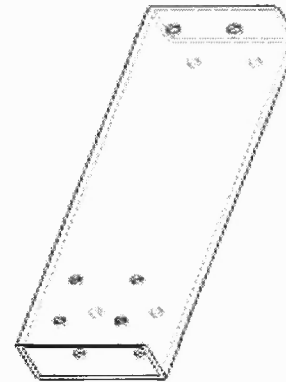
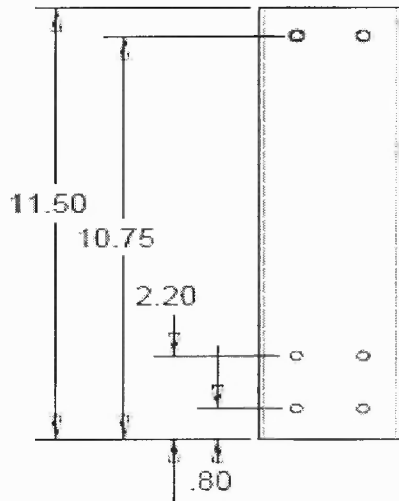


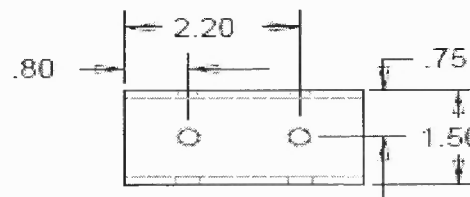
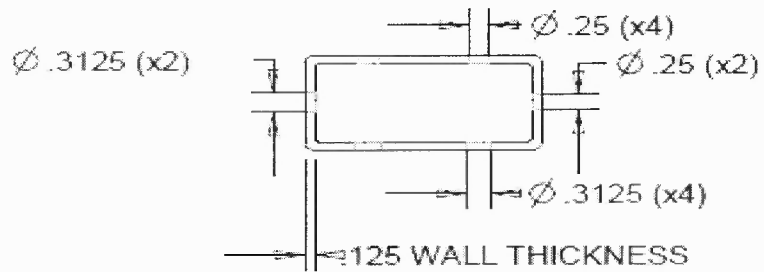
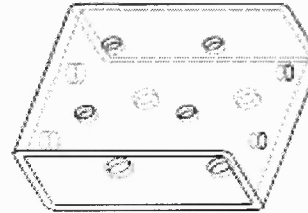
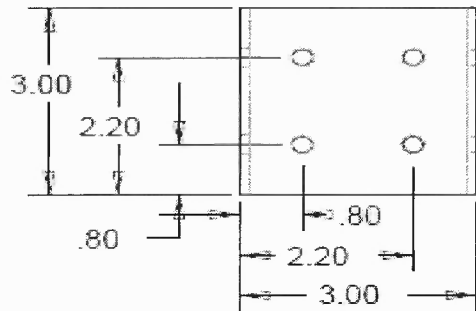
Figure G.6 Vertical support tube #2 drawing.



ALL DIMENSIONS IN INCHES

Title VERTICAL MOUNTING TUBE			Part Number 1011
Drawn Jon Weimer	Date 10/03/2009	Sheet 1 of 1	Material Aluminum

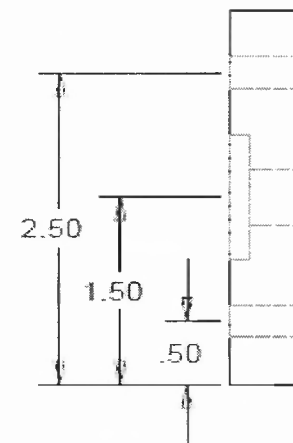
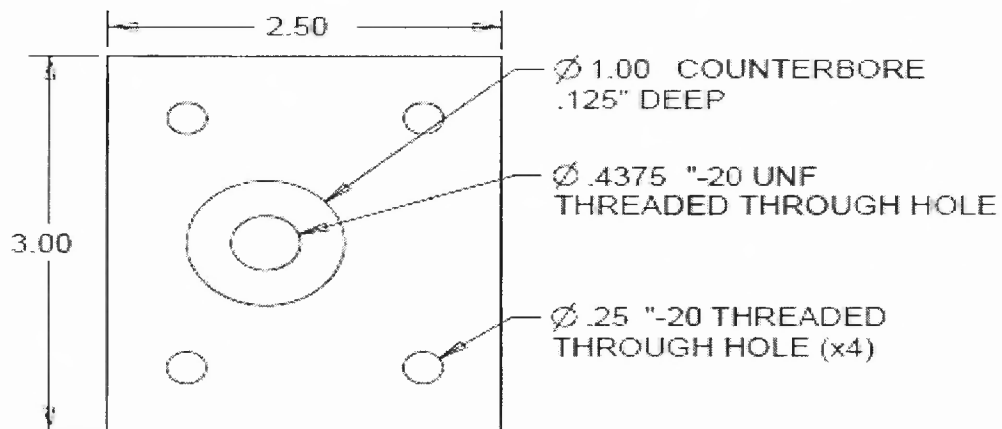
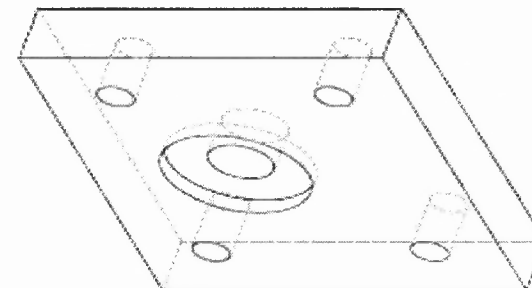
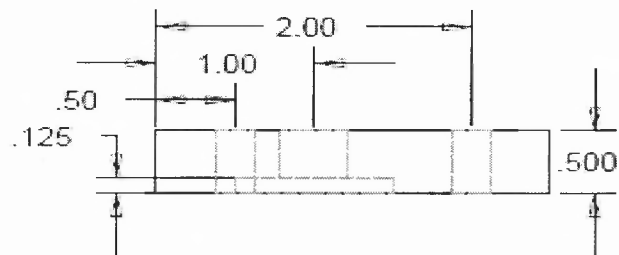
Figure G.7 Vertical mounting tube drawing.



ALL DIMENSIONS IN INCHES

Title CONNECTING TUBE			Part Number 1012
Drawn Jon Weimer	Date 10/03/2009	Sheet 1 of 1	Material Aluminum

Figure G.8 Connecting tube drawing.



ALL DIMENSIONS IN INCHES

Title PISTON MOUNTING BRACKET			Part Number 1035
Drawn Jon Weimer	Date 10/03/2009	Sheet 1 of 1	Material Aluminum

Figure G.9 Piston mounting bracket drawing.

APPENDIX H

MATLAB CODE

This Appendix contains the three programs that were designed for the three loading scenarios described earlier in this thesis: 0 lb, 90 lbs, and 180 lbs. Following is the code for the 0 lb loading condition. The program is identical for all loading cases, with the exception of a single parameter. The amount of time allotted for free-fall decreases with increasing weight. Shown below, the length of the pause is 0.15 seconds for free-fall. For the 90 lbs loading case, the length of the pause is 0.08 seconds. Finally, when the device is loaded with 180 lbs, the length of the pause is 0.05 seconds.

```
%%%%%%%%%%%%%%%%%%%%%%%%%%%%%%%%%%%%%%%%%%%%%%%%%%%%%%%%%
clear all
clc

% Create I/O adapters for cylinder control.
dio=digitalio('nidaq','Dev1'); %Digital adapter
ai=analoginput('nidaq','Dev1'); %Analog adapter
% Adding lines to the I/O adapter. Specify the adapter, the
% numeric IDs of the hardware lines added, the port number, the direction,
% and name the lines.
cline=addline(dio,0:7,'out'); %Digital channels
chan=addchannel(ai,0); %Analog channels
duration=60.0000; %60 second acquisition

%Analog data parameters
Fs = 1000; %Sample Rate
ai.Channel.InputRange = [-10 10]; %Analog Input Range
set(ai,'SampleRate',Fs)
ActualRate=get(ai,'SampleRate'); %Actual Sample Rate
set(ai,'ManualTriggerHwOn','Start') %Trigger immediately after "Start" command
set(ai,'SamplesPerTrigger',inf) %Continually sample
set(ai,'InputType','SingleEnded') %Single-ended analog data
blocksize=get(ai,'SamplesPerTrigger');
Fs=ActualRate;
```

```

%Filter Parameters
Fc =6; %Cutoff Frequency

tic
time=toc;
start(ai) %Start analog device
pause(2)
putvalue(dio,[1 0 0 0 0 0 0]) %Rising
pause(3)
while (time<duration)
    putvalue(dio,[0 1 0 0 0 0 0]) %Free-falling
    pause(0.15)
    putvalue(dio,[1 0 0 0 0 0 0]) %Rising
    pause(3)
    time=toc;
end

q=ai.SamplesAvailable; %Number of Samples Available
[data_unfiltered,time]=getdata(ai,q); %[volts,seconds]
data_unfiltered_inches=(data_unfiltered/max(data_unfiltered))*4; %Inches
putvalue(dio,[0 0 0 0 0 0 0]) %Shutdown Process

%Filter Data
[B,A] = butter(2,2*Fc/Fs);
data_filtered = filtfilt(B,A,data_unfiltered_inches); %Inches

%Central Difference Method
for i=1:q
    if i == 1
        vel_data(i,1) = (data_filtered(i+1) - data_filtered(i))/(time(i+1) - time(i)); %in/s
    elseif i < q
        vel_data(i,1) = (data_filtered(i+1) - data_filtered(i-1))/(time(i+1) - time(i-1)); %in/s
    else
        vel_data(i,1) = (data_filtered(i) - data_filtered(i-1))/(time(i) - time(i-1)); %in/s
    end
end

for j=1:q
    if j == 1
        acc_data(j,1) = (vel_data(j+1) - vel_data(j))/(time(j+1) - time(j))/12; %ft/s^2
    elseif j < q
        acc_data(j,1) = (vel_data(j+1) - vel_data(j-1))/(time(j+1) - time(j-1))/12; %ft/s^2
    else
        acc_data(j,1) = (vel_data(j) - vel_data(j-1))/(time(j) - time(j-1))/12; %ft/s^2
    end
end
end

```

```
stop(ai) %Stop analog device
delete(ai) %Delete analog device
clear ai
```

```
%Plot Results
```

```
figure(1)
plot(time,data_filtered,'k','linewidth',1)
```

```
figure(2)
plot(time,vel_data,'b','linewidth',1)
```

```
figure(3)
plot(time,acc_data,'r','linewidth',1)
```

```
figure(4)
plot(time,data_unfiltered_inches,'k','linewidth',1)
```

```
%%%%%%%%%%
```

REFERENCES

- [1] Fee JW, Samworth KT. Passive leg motion changes in cerebral palsied children after whole body vertical accelerations. *IEEE Trans Rehab Eng.* 1995;3(2):228-232.
- [2] Fong K. The next small step. *BMJ.* 2004;329:1441-1444.
- [3] Clement G, Moore ST, Raphan T, Cohen B. Perception of tilt (somatogravic illusion) in response to sustained linear acceleration during space flight. *Exp Brain Res.* 2001;138:410-418.
- [4] Clement G, Gurfinkel V, Lestienne F, Lipshits MI, Popov KE. Adaptation of postural control to weightlessness. *Exp Brain Res.* 1984;57:61-72.
- [5] Cordo PJ, Nashner LM. Properties of postural adjustments associated with rapid arm movements. *J Neurophysiol.* 1982;47:287-302.
- [6] Massion J, Gurfinkel V, Lipshits M, Obadia A, Popov K. Axial synergies under microgravity conditions. *J Vestib Res.* 1993;3:275-287.
- [7] Lackner JR, DiZio P. Motor function in microgravity: movement in weightlessness. *Curr Opin Neurobiol.* 1996;6:744-750.
- [8] McDonald PV, Basdogan C, Bloomberg JJ, Layne CS. Lower limb kinematics during treadmill walking after space flight. Implications for gaze stimulation. *Exp Brain Res.* 1996;112:325-331.
- [9] Bloomberg JJ, Peters BT, Huebner WP, Smith SL, Reschke MF. Locomotor head-trunk coordination strategies following space flight. *J Vestib Res.* 1997;7(2-3):161-177.
- [10] Paloski WH, Bloomberg JJ, Reschke MF, Harm DL. Space flight induced changes in posture and locomotion. *J Biomech.* 1994;27:812-815.
- [11] di Prampero PE, Narici MV, Tesch PA. A world without gravity: Muscles in space. *ESA Special Publication.* 2001;(SP-1251):69-82.
- [12] The University of Western Ontario. Department of Physiology and Pharmacology [Internet]. The physiology of the senses. Lecture 10-balance; [cited 2009 Oct 13]; [9 pages]. Available from: <http://www.physpharm.fmd.uwo.ca/undergrad/sensesweb/L10Balance/L10Balance.pdf>.
- [13] Farber SD. *Neurorehabilitation: A multisensory approach.* Philadelphia: Saunders. 1982;132-144.

- [14] Fiebert IM, Brown E. Vestibular stimulation to improve ambulation after cerebral vascular accident. *Phys Ther.* 1979;59(4):423-426.
- [15] Trombly CA. *Occupational therapy for physical dysfunction.* Baltimore: Williams & Wilkins. 1984;65-66.
- [16] Donahue K. Horses can provide therapeutic benefits. *OT Week.* 1984;4-5.
- [17] Wartenburg R. Pendulousness of legs as a diagnostic test. *Neurol.* 1951;1:1824-1830.
- [18] Black FO et al. Disruption of postural readaptation by inertial stimuli following space flight. *J Vestib Res.* 1999;9:369-378.
- [19] Mead Fluid Dynamics, Inc; c2009 [Internet]. Control valves; [cited 2009 Nov 8]; [9 pages]. Available from: <http://www.mead-usa.com/media/mod3.pdf>.
- [20] Alkon Corp; c2006 [Internet]. Directional control air valves & accessories; [cited 2009 Nov 8]; [88 pages]. Available from: <http://www.alkoncorp.com/pdf/ALKON%20VALVE%20CATALOG%202005.pdf>.
- [21] National Instruments Corp; c2009 [Internet]. NI DAQCard-6024E (for PCMCIA); [cited 2009 Nov 8]; [5 pages]. Available from: <http://sine.ni.com/nips/cds/print/p/lang/en/nid/10969>.
- [22] National Instruments Corp; c2009 [Internet]. Multifunction DAQ accessory and cable selection guide; [cited 2009 Nov 8]; [5 pages]. Available from: <http://www.ni.com/pdf/products/us/4daqsc212.pdf>.
- [23] Wikipedia [Internet]. MATLAB:CB-68LP pinout; [modified 2009 Jan 29; cited 2009 Nov 8]; [2 pages]; Available from: http://pundit.pratt.duke.edu/wiki/MATLAB:CB-68LP_Pinout.
- [24] RadioShack Corp; c2009 [Internet]. Compact 5VDC/1A SPST reed relay; [cited 2009 Nov 8]; [2 pages]. Available from: <http://www.radioshack.com/product/index.jsp?productId=2062478&tab=summary>.
- [25] Bimba Manufacturing Company; c2009 [Internet]. Position control system products; [cited 2009 Nov 9]; [54 pages]. Available from: http://www.bimba.com/pdf/catalogs/FL_PCS.pdf#page=3.